Heliyon 10 (2024) e31760

Contents lists available at ScienceDirect

Heliyon

journal homepage: www.cell.com/heliyon

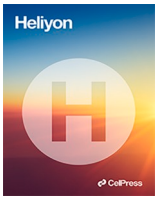

Research article

A holistic exploration of the optimal control strategies on an enhanced mathematical model for the co-infection of HIV/AIDS and varicella-zoster

Belela Samuel Kotola [a,*], Shewafera Wondimagegnhu Teklu [b]

[a] Department of Mathematics, Oda Bultum University, Chiro, Ethiopia
[b] Department of Mathematics, Natural and Computational Sciences, Debre Berhan University, Ethiopia

ARTICLE INFO

Keywords:
Varicella-zoster virus
HIV/AIDS
Treatment
Vaccination
Co-infection

ABSTRACT

Because of its high contagiousness and correlation with HIV/AIDS complaints, the virus that causes varicella-zoster virus and its interactions have major consequences for a considerable portion of people worldwide. The primary aim of this work is to suggest and examine optimal control methods for managing the transmission dynamics of HIV/AIDS and Varicella-Zoster co-infection, using an integer model approach. The mathematical analyses of the proposed integer order model places particular emphases on the boundedness and non-negativity of the model solutions, scrutinizing equilibrium points, determining the models basic reproduction ratios (the models basic reproduction numbers) through the next-generation matrix operator method, and assessing the model equilibrium points existences and stabilities in local approach by considering the local stability conditions of Routh and Hurwitz. Additionally, it incorporates an optimal control framework to enhance our understanding of the dynamics involved in the spreading of HIV/AIDS and Varicella-Zoster co-infection within a considered population. This entails determining preventative measures that can be deliberately put into place to lessen the effects of these co-infections. The solutions of the HIV/AIDS and Varicella-Zoster co-infection model converges to the co-infection endemic equilibrium point whenever the associated basic reproduction number is greater than unity, as verified by numerical simulation results. Including optimal management gives the research an innovative viewpoint and helps identify tactical ways to mitigate the negative effects of this co-infection on the public health. The results highlight how crucial it is to address these complex structures in order to protect and improve public health outcomes. Implementing the proposed protection measures and treatment measures simultaneously has most effective result to minimize and eliminate the HIV/AIDS and Varicella-Zoster co-infection disease throughout the population.

1. Introduction

Health-harming microorganisms like bacteria, fungi, viruses, or parasites can spread infectious diseases, often known as common illnesses, which are transmittable from one host to another in several different ways including droplets of aerosol, water-borne routes, food-borne pathways, through vectors, or during birth from mother to baby [1–3]. The virus known as varicella-zoster abbreviated as

* Corresponding author.
E-mail address: belelasamuel@gmail.com (B.S. Kotola).

https://doi.org/10.1016/j.heliyon.2024.e31760
Received 10 October 2023; Received in revised form 20 May 2024; Accepted 21 May 2024
Available online 22 May 2024

VZV is the etiological agent responsible for both shingles and varicella (commonly known as chickenpox) clinically termed as herpes-zoster. The transmission dynamics of the virus called varicella-zoster involve the dissemination primarily through respiratory droplets and direct contact with actively shedding herpes-zoster lesions [4–7]. Furthermore, it is of significance to highlight that the virus called varicella-zoster, acting as the primary presentation of the ailment, can undergo reactivation in individuals concurrently afflicted with human immunodeficiency virus (HIV) infection. This dynamic interplay underscores the intricate association between these two viral agents and the complexities that emerge within the framework of an impaired immune system [8,9].

Acute or chronic lytic infections caused by several viral agents, particularly herpes viruses, might manifest immune deficits before the onset of AIDS symptoms. Varicella-zoster stands out among them as a viral agent that can be reactivated by immunological changes in an HIV-positive patient [10]. There are various possibilities for the co-existence of HIV/AIDS and varicella-zoster in an individual that means immunosuppression human immunodeficiency virus/acquired immune deficiency syndrome (HIV/AIDS) has been associated with a significantly increased risk of varicella-zoster reactivation [11,12].

Co-infection entails the simultaneous presence of two distinct disease strains or disease pathogens, occurring concurrently or within a close temporal proximity before the initial strain or pathogen establishes infection and elicits an immune response. Additionally, it denotes the infection of a singular host by multiple variants (strains) of a pathogen or by discrete species of pathogens. Notably, co-infection with multiple pathogen strains is frequently observed in pneumonia, underscoring its prevalence across various disease contexts [13].

Individuals with certain levels of CD4 cells and no detectable virus in their blood after a year of treatment tend to live as long as others [13,14]. Such treatment significantly diminishes the presence of HIV in bodily fluids, often leading to it becoming practically non-existent, a state referred to as being 'undetectable.' Consequently, when an individual consistently adheres to their antiretroviral medication regimen and maintains an undetectable viral load, the risk of transmitting the virus to a sexual partner without HIV is effectively eliminated [15].

Research scholars across different countries throughout countries in the world have investigated the co-interaction of COVID-19 with several infectious diseases, including tuberculosis (TB), HIV/AIDS, HBV, and cholera refer studies [13,16–20]. The studies carried out in Refs. [10,13,16,17,19–25], formulated and analyzed the spreading dynamics of infectious diseases using compartmental integer order modeling approach, studies carried out in Refs. [18,26–32], formulated and examined the spreading dynamics of infectious diseases using fractional order modeling approach. Investigating and predicting the spreading rates of infectious diseases using compartmental modeling approaches has fundamental effects to tackle the spreading problem in the community [25]. In order to develop and analyze the compartmental integer order model for HIV/AIDS and varicella-zoster co-infection, it is essential to acquire fundamental concepts, methodologies, and epidemic characteristics of infectious diseases through a mathematical modeling approach. Therefore, we have conducted a thorough review of relevant research literature conducted by scholars across various countries worldwide.

In [25], an author explored optimal control strategies for managing the COVID-19 and malaria co-epidemic through the development of a compartmental model. Their findings indicate that the simultaneous implementation of protective measures offers the most effective means of minimizing the co-epidemic within the population. Similarly, another researcher [18] devised a model for pneumonia and HIV/AIDS co-infection, assessing the impacts of treatment and vaccination strategies in controlling transmission. Furthermore [19], examined the effects of preventive measures on cholera and COVID-19 co-infection in Yemen using compartmental modeling techniques. Additionally, the research paper [20] established a compartmental model to analyze the spread of HIV and pneumonia co-epidemics within communities, exploring strategies for controlling transmission.

In this research work, we found that previous studies on infectious diseases did not explore the effects of time-dependent optimal control strategies on the co-infection of HIV/AIDS and Zoster- Virus. This gap in existing research inspired us to focus on this aspect in our study, making our model novel compared to previous ones. Therefore, our main goal is to investigate how optimal control strategies can predict and manage the spread of the HIV/AIDS and varicella-zoster virus co-infection within communities. We aim to achieve this by developing a new model specifically for this co-epidemic. The remaining sections of this proposed study are structured as: section 2 revealed that all the descriptions, assumptions and necessary steps for the HIV/AIDS and varicella-zoster co-infection model construction, section 3 given us the mathematical analysis of the constructed models, section 4 constructed and analyzed optimal problem of the co-infection model, section 5 analyzed the sensitivity of the co-infection model parameters and carried out the numerical simulations of the model and section 6 concluded the basic concepts of the research study.

2. The HIV/AIDS and varicella-zoster Co-infection model construction

2.1. Descriptions and assumptions for the proposed model

Let us represent the compartments involved in the proposed HIV/AIDS and Varicella-Zoster virus co-infection model as: $S(t)$ be the total number of people who are at risk (susceptible) for both the HIV/AIDS and varicella-zoster infections, $H(t)$ be the total number of people who are attacked (infected) by HIV, $P(t)$ be the total number of people who are infected with zoster, $C(t)$ be the total number of co-infected people with HIV/AIDS and varicella-zoster, $A(t)$ be the total number of people who have undetected viral load, $V(t)$ be the total number of people who are vaccinated against zoster infection, and $T(t)$ be the total number of people who got zoster treatment in order that the total population involved in the proposed study is represented by

$$N(t) = S(t) + H(t) + P(t) + C(t) + A(t) + V(t) + T(t). \tag{1}$$

Important assumptions:

- ➢ Population distribution is in a uniform manner in each compartment.
- ➢ People who have undetectable viral loads do not spread the infection to others.
- ➢ Individuals in each compartment are subjected to natural mortality rate.
- ➢ The total number of human population is not constant.
- ➢ There is no dual infection simultaneous transmission.
- ➢ Vertical transmission of HIV is taken into account.
- ➢ There is no permanent immunity to zoster infection.
- ➢ There is waning of zoster vaccination effectiveness.
- ➢ Due to HIV/AIDS infection's potential to weaken the immune system there's an increased risk of zoster virus reactivation.
- ➢ Because HIV/AIDS and Zoster are viral infections that will have chronic stages people who are susceptible are at risk for HIV/AIDS or zoster infections acquire HIV and zoster respectively at the standard incidence rate represented by

$$f_1(t) = \frac{\alpha_1}{N}(H(t) + \varepsilon_1 C(t)), \tag{2}$$

$$f_2(t) = \frac{\alpha_2}{N}(P(t) + \varepsilon_2 C(t)), \tag{3}$$

where $\varepsilon_1, \varepsilon_2 \geq 1$ are parameters that reveals the degree of individuals infectiousness and

α_1 and α_2 are the spreading rates of HIV/AIDS and varicella-zoster respectively.

Based on the model state variables, the model assumptions described in the sub-section 2.1 and the model parameters interpreted in Table 1 above the population flow diagram for the HIV/AIDS and varicella-zoster co-infection spreading dynamics is represented Fig. 1.

Using the population flow diagram given by Fig. 1 above that represent the co-infection spreading dynamics is represented by the following systems of ordinary differential equations:

$$\begin{aligned}
\frac{dS}{dt} &= (1-p)\Delta + \kappa V - (f_1 + f_2 + d)S,\\
\frac{d\mathrm{V}}{dt} &= p\Delta - (\kappa + \mathrm{d})\mathrm{V},\\
\frac{d\mathrm{H}}{dt} &= f_1 S + (1-\psi)\varphi H - (\delta_1 f_2 + \theta_2 + d_2 + \mathrm{d})\mathrm{H},\\
\frac{d\mathrm{P}}{dt} &= f_2 S + \sigma T - (\delta_2 f_1 + \theta_1 + d_1 + \mathrm{d})\mathrm{P},\\
\frac{d\mathrm{C}}{dt} &= \delta_1 f_2 H + \delta_2 f_1 P + \rho A - (\theta_3 + d_3 + d)\mathrm{C},\\
\frac{d\mathrm{A}}{dt} &= \theta_2 \mathrm{H} + \theta_3 \mathrm{C} - (\rho + d)\mathrm{A},\\
\frac{d\mathrm{T}}{dt} &= \theta_1 P - (\sigma + d)T,
\end{aligned} \tag{4}$$

Table 1
Biological interpretations of parameters incorporated in the co-infection model.

Parameter	Interpretations of parameters per unit of time
d	The rate at which individuals died naturally
Δ	The rate at which individuals are recruited
p	The portion of recruited individuals who have got zoster vaccination
κ	The rate at which zoster vaccination wanes
δ_1	The parameter that modify individuals infectiousness
δ_2	The parameter that modify individuals infectiousness
d_1	The rate at which individuals died with zoster infection
d_2	The rate at which unaware HIV infected individuals died with HIV infection
d_3	The rate at which individuals died with HIV/AIDS and varicella-zoster co-infection
$\boldsymbol{\sigma}$	The rate at which individuals recovered from zoster infection are re-infected
ρ	The rate at which infected individuals with undetectable viral load become re-infected by zoster
α_1	The rate at which individuals spread HIV/AIDS
α_2	The rate at which individuals spread varicella-zoster
θ_1	The rate at which individuals treated from varicella-zoster infection
θ_2	The rate at which individuals treated from HIV/AIDS infection
θ_3	The rate at which individuals treated from HIV/AIDS and varicella-zoster co-infection
ψ	The death probability of newborns infected with HIV during birth
$\boldsymbol{\varphi}$	The rate at which HIV spreads from mother to child during birth

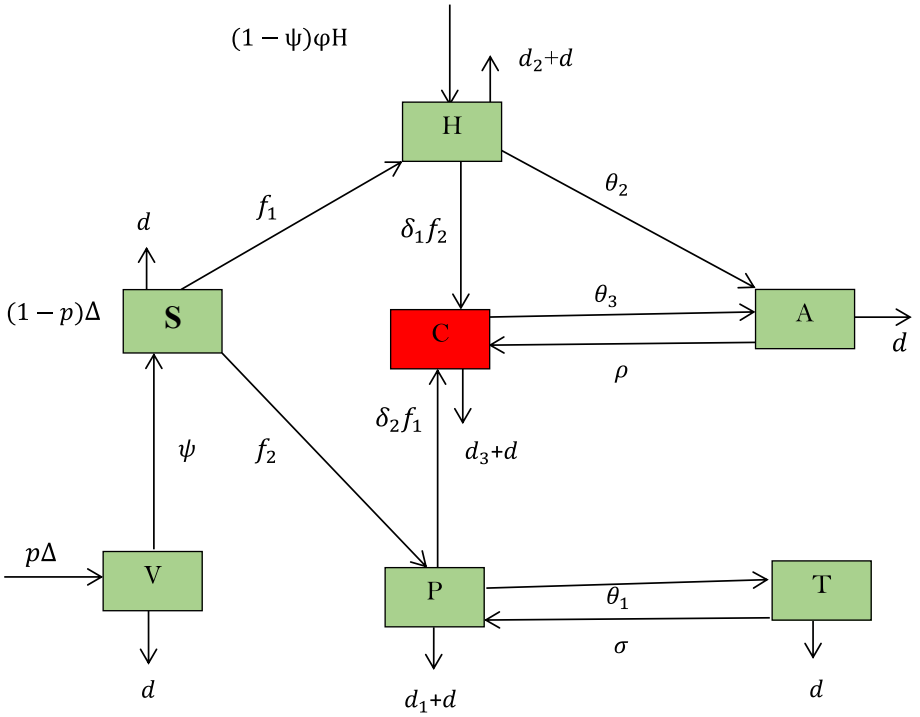

Fig. 1. The population flow diagram such that f_1 and f_1 are represented by equations (2) and (3) respectively.

with the corresponding initial population $S(0) = S^0 \geq 0, V(0) = V^0 \geq 0, P(0) = P^0 \geq 0, H(0) = H^0 \geq 0, A(0) = A^0 \geq 0, T(0) = T^0 \geq 0$ and $N(t)$ is described in equation (1).

3. Mathematical analyses of the Co-infection model (4)

3.1. Properties of the co-infection model (4) solutions

The two most important properties of an epidemiological model that should be proved are the uniqueness, non-negativity and boundedness for the model solutions.

Theorem 1. *The HIV/AIDS and Varicella-Zoster co-infection dynamical system* (4) *solutions are exists, unique, non-negative and bounded in the set described by*

$$\Omega = \left\{(S, V, H, P, C, A, T) \epsilon\ \mathbb{R}_+^7 : 0 \leq N \leq \frac{\Delta}{d}\right\}. \tag{5}$$

Proof. To prove Theorem 1 stated above let us apply the theorem stated and proved by Picard–Lindelöf see reference [33]. This theorem is the most common approach to prove the ordinary differential equations (the initial value problem) solutions will exist and unique, where the functions incorporated are Lipschitz continuous locally. In our scenario, the functions defined on the co-infection model (4) right-hand side part are C^1 on the topology of $\mathbb{R}_+^7$, at which Picard–Lindelöf criteria holds. Hence, the solution for the HIV/AIDS and varicella-zoster co-infection dynamical system (4) uniquely exist.

According to the criteria stated by proposition A.1 of the research literature [34] one can verify that the functions in the co-infection model (4) described in the right hand side by $g_i(S, V, H, P, C, A, T)$ are non-negative provided that $y \in [0, \infty)^7$ and $y_i = 0$. This proved the theorem and is fundamental characteristic, particularly in mathematical epidemiology models, where negativity for the population state variables is meaningless.

Boundedness for the HIV/AIDS and varicella-zoster co-infection model (4) solution is the necessary and sufficient condition to reveals that the co-infection model solutions remain within a certain specified region. One can verified as the constructed functions described in the right hand side of the model (4) by $g_i(S, V, H, P, C, A, T)$ holds the property $g_i(S, V, H, P, C, A, T) \geq 0$, as indicated in proposition A.1.

According to non-negativity conditions and the criteria of theorem stated by Picard–Lindelöf t the HIV/AIDS and varicella-zoster co-infection model (4) solutions remained in the region described by $[0, \infty)^7$ for each time $t \geq 0$. The total sum of all the differential equations described in the co-infection model (4)gives the result $\frac{dN}{dt} \leq \Delta - dN$. Thus, we determined the total number of human

population denoted by N(t) and stated in equation (1) as $N(t) \leq N_0 e^{-dt} + \frac{\Delta}{d}\left(1 - e^{-dt}\right)$ which implies $N(t)$ is converges in the range of $[0, \frac{\Delta}{d}]$. Consequently, the HIV/AIDS and varicella-zoster co-infection model (4) solution uniquely exist, and bounded in the region Ω as defined in equation (5).

3.2. The co-infection model disease-free equilibrium point

The HIV/AIDS and Varicella-Zoster co-infection model (4) disease-free equilibrium point denoted by (E^0_{HZ}) is computed in the absence of both HIV/AIDS and varicella-zoster diseases within the population such that $H = P = C = A = T = 0$ and by putting system (4) equal to zero. Thus, after simplifying the computations the required co-infection disease-free equilibrium point for the co-infection model (4) is represented by:

$$E^0_{HZ} = (S^0, V^0, H^0, P^0, C^0, A^0, T^0) = \left(\frac{(\kappa + d)(1-p)\Delta + p\Delta\kappa}{(\kappa + d)d}, \frac{\Delta p}{\kappa + d}, 0, 0, 0, 0, 0\right). \tag{6}$$

3.3. The co-infection model (4) effective reproduction number

An epidemiological model basic reproduction ratio represented by $\mathscr{R}_0$, is a measure of how many new cases an average infected person can produce in a population where everyone is susceptible [17,35] whereas the effective reproduction number is the average secondary infected individuals produced by a single infected person in some susceptible and some non-susceptible population. Based on the criteria applied in Ref. [36], let's define $\mathscr{V}^+_i(x)$ as the rate of people entering compartment i, $\mathscr{V}^{-1}_i(x)$ as the rate of people leaving compartment i, and $\mathscr{F}_i(x)$ as the rate at which new cases of the disease occur in compartment i. Then $\mathscr{V}_i(x) = \mathscr{V}^-_i(x) - \mathscr{V}^+_i$, $F = \left[\frac{\partial \mathscr{F}_i}{\partial X_j}(X_o)\right]$ and $V = \left[\frac{\partial \mathscr{V}_i}{\partial X_j}(X_o)\right]$, where F and V are mxm matrix with m is number of infected compartment and the product F V^{-1} is known as the next-generation matrix. The dominant eigenvalue in magnitude of F V^{-1} represents the basic/effective reproduction number as computed in Refs. [17,35]. In this sub-section, we need to compute three reproduction ratios (reproduction numbers) incorporated in the co-infection model (4).

3.3.1. Basic reproduction number for HIV/AIDS only infection

Now consider the HIV/AIDS and varicella-zoster co-infection model (4) and compute the HIV/AIDS only infection basic reproduction number as.

$$\mathscr{F}_i(x) = \begin{bmatrix} f_1 S \\ 0 \end{bmatrix} \text{ and } \mathscr{V}_i(x) = \begin{bmatrix} (\theta_2 + d_2 + d)H - (1-\psi)\varphi H \\ (\rho + \mu)A - \theta_2 H \end{bmatrix}.$$

At the HIV/AIDS disease-free equilibrium point described in equation (6) where $H = A = 0$ we have determined the results represented by

$$N^0 = S^0, F = \begin{bmatrix} \alpha_1 & \alpha_1 \\ 0 & 0 \end{bmatrix}, V = \begin{bmatrix} \theta_2 + d_2 + d - (1-\psi)\varphi & 0 \\ -\theta_2 & \rho + d \end{bmatrix},$$

and

$$V^{-1} = \begin{pmatrix} \frac{1}{\theta_2 + d_2 + \mu - (1-\psi)\varphi} & 0 \\ \frac{\tau_2}{(\theta_2 + d_2 + \mu)(\rho + d) - (\rho + d)(1-\psi)\varphi} & \frac{1}{\rho + d} \end{pmatrix}.$$

Then we have computed the two matrices product represented by

$$FV^{-1} = \begin{pmatrix} \left(\frac{\alpha_1}{\rho + d}\right)\frac{(\rho + d + \tau_2)}{(\theta_2 + d_2 + d) - (1-\sigma)\varphi} & \frac{\alpha_1}{\rho + d} \\ 0 & 0 \end{pmatrix}.$$

Thus, the HIV/AIDS only infection basic reproduction number is denoted represented by

$$\mathscr{R}_1 = \frac{\alpha_1(\rho + d + \theta_2)}{(\rho + d)((\theta_2 + d_2 + d) - (1-\sigma)\varphi)}. \tag{7}$$

3.3.2. The varicella-zoster effective reproduction number

Using similar approach used in the sub-section 3.3.1, the varicella-zoster disease-free equilibrium point and the co-infection model (4) we determined the results given by

$$\mathscr{F}_i(x) = [f_2 S] \text{ and } \mathscr{V}_i(x) = (\theta_1 + d_1 + \mathrm{d})\mathrm{P},\ N^0 = S^0 + V^0, F = \frac{\alpha_2(\kappa + \mathrm{d})d}{(\kappa + \mathrm{d})(1-p) + p\kappa + pd},$$

$$V = (\theta_1 + d_1 + \mathrm{d}), \text{and } V^{-1} = \frac{1}{\theta_1 + d_1 + \mathrm{d}}.$$

Thus, we have also got the product given by $FV^{-1} = \frac{\alpha_2(\kappa+\mathrm{d})d}{[(\kappa+\mathrm{d})(1-p)+p\kappa+pd](\theta_1+d_1+\mathrm{d})}$ and the varicella-zoster only infection effective reproduction number is denoted and represented by

$$\mathscr{R}_2 = \frac{\alpha_2(\kappa + \mathrm{d})d}{[(\kappa + \mathrm{d})(1-p) + p\kappa + pd](\theta_1 + d_1 + \mathrm{d})}. \tag{8}$$

3.3.3. Effective reproduction number for the Co-infection model

By applying similar criteria in the sub-sections 3.3.1 and 3.3.2 the HIV/AIDS and varicella-zoster co-infection model (4) effective reproduction is computed as follows:

$$\mathscr{F}_i(x) = \begin{bmatrix} f_1 S \\ f_2 S \\ 0 \\ 0 \end{bmatrix} \text{ and } \mathscr{V}_i(x) = \begin{bmatrix} (\delta_1 f_2 + \theta_2 + d_2 + \mathrm{d})\mathrm{H} - (1-\sigma)\varphi H \\ (\delta_2 f_1 + \theta_1 + d_1 + \mathrm{d})\mathrm{Z} - \sigma T \\ (\,\theta_3 + d_3 + \mu)\mathrm{C} - \alpha f_2 H - \delta_2 f_1 P - \rho A \\ (\rho + d)\mathrm{A} - \theta_2 \mathrm{H} - \theta_3 \mathrm{C} \end{bmatrix},$$

and computation at the co-infection model (4) disease-free equilibrium point E^0_{HC} gives the results illustrated by

$$N^0 = S^0 + V^0, F = \begin{bmatrix} \frac{\alpha_1 S}{N} & 0 & \frac{\alpha_1 S}{N} & \frac{\alpha_1 S}{N} \\ 0 & \frac{\alpha_2 S}{N} & \frac{\alpha_2 S}{N} & 0 \\ 0 & 0 & 0 & 0 \\ 0 & 0 & 0 & 0 \end{bmatrix},$$

$$V = \begin{bmatrix} (\theta_2 + d_2 + \mathrm{d}) - (1-\sigma)\varphi & 0 & 0 & 0 \\ 0 & (\theta_1 + d_1 + \mathrm{d}) & 0 & 0 \\ 0 & 0 & (\,\theta_3 + d_3 + d) & -\rho \\ -\theta_2 & 0 & -\theta_1 & (\rho + d) \end{bmatrix},$$

$$V^{-1} =$$

$$\begin{pmatrix} \frac{1}{d-(1-\sigma)\varphi + d_2 + \theta_2} & 0 & 0 & 0 \\ 0 & \frac{1}{\theta_1 + d_1 + \mathrm{d}} & 0 & 0 \\ \frac{\rho\theta_2}{(d-(1-\sigma)\varphi + d_2 + d\theta_2)(d^2 + d\rho + dd_3 + \rho d_3 + d\theta_3)} & 0 & \frac{d+\rho}{d^2 + d\rho + dd_3 + \rho d_3 + d\theta_3} & \frac{\rho}{d^2 + d\rho + dd_3 + \rho d_3 + d\theta_3} \\ \frac{\theta_2(d + d_3 + \theta_3)}{(d-(1-\sigma)\varphi + d_2 + \theta_2)(d^2 + d\rho + dd_3 + \rho d_3 + d\theta_3)} & 0 & \frac{\theta_3}{d^2 + d\rho + dd_3 + \rho d_3 + d\theta_3} & \frac{d + d_3 + \theta_3}{d^2 + d\rho + dd_3 + \rho d_3 + d\theta_3} \end{pmatrix},$$

and

$$FV^{-1} = \begin{pmatrix} \frac{\delta_1}{d-(1-\sigma)\varphi + d_2 + \theta_2} & 0 & 0 & 0 \\ 0 & \frac{\delta_2}{d + d_1 + \theta_1} & 0 & 0 \\ 0 & 0 & 0 & 0 \\ 0 & 0 & 0 & 0 \end{pmatrix}.$$

Therefore, the characteristics polynomial of the matrix FV^{-1} gives the eigenvalues illustrated by $\left\{0, 0, \frac{\frac{\alpha_1 S}{N}}{d-\varphi+\sigma\varphi+d_2+\theta_2}, \frac{\frac{\alpha_2 S}{N}}{d+d_1+\theta_1}\right\}$.

Thus, the HIV/AIDS and varicella-zoster co-infection model (4) effective reproduction number is denoted and represented by

$$\mathscr{R}_{ef} = max\left\{ \frac{(\mathrm{d}(1-\mathrm{p})+\kappa)\alpha_1}{(d+\kappa)(d-\varphi+\sigma\varphi+d_2+\theta_2)}, \frac{(d(1-p)+\kappa)\alpha_2}{(d+\kappa)(d+d_1+\theta_1)} \right\}. \tag{9}$$

3.3.4. The model (4) disease-free equilibrium point and its stability

Theorem 2. The HIV/AIDS and varicella-zoster co-infection model disease-free equilibrium point $\mathrm{E}^0_{\mathrm{HC}}$ has a local asymptotic stability whenever the associated co-infection effective reproduction number described in the equation (9) is less than unity means $\mathscr{R}_{\mathrm{ef}} < 1$ and is unstable whenever $\mathscr{R}_{\mathrm{ef}} > 1$.

Proof. *The matrix denoted by $J(E^0_{HZ})$ and known as the Jacobian matrix for the HIV/AIDS and varicella-zoster co-infection dynamical system* (4) *at the model disease-free equilibrium point E^0_{HZ} is computed and represented as*

$$J(E^0_{HZ}) = \begin{bmatrix} -d & \kappa & -a & -bS & -a\omega_1 - b\omega_2 & -a & 0 \\ 0 & -\mathrm{c} & 0 & 0 & 0 & 0 & 0 \\ 0 & 0 & m & 0 & 0 & 0 & 0 \\ 0 & 0 & 0 & -\mathrm{e} & 0 & 0 & \sigma \\ 0 & 0 & 0 & 0 & -\mathrm{f} & \rho & 0 \\ 0 & 0 & \theta_2 & 0 & \theta_3 & -\mathrm{g} & 0 \\ 0 & 0 & 0 & \theta_1 & 0 & 0 & -h \end{bmatrix},$$

where, $\mathrm{a} = \frac{\alpha_1}{N}S$, $\mathrm{b} = \frac{\alpha_2}{N}S$, $\mathrm{c} = (\kappa + d)$, $\mathrm{m} = (1-\sigma)\varphi - (\theta_2 + d_2 + \mathrm{d})$, $\mathrm{e} = (\theta_1 + d_1 + \mathrm{d})$,

$\mathrm{f} = (\theta_3 + d_3 + d), \mathrm{g} = (\rho + d), \mathrm{h} = (\sigma + \mathrm{d})$.

Then Characteristic equation of the matrix $J(E^0_{HZ})$ at the disease-free equilibrium point E^0_{HZ} is computed and represented by

$$(-c-\lambda)(m-\lambda)(-\lambda+d-)\big((-e-\lambda)(-h-\lambda)\big(gx+\lambda^2-fg+f\lambda+\rho\theta_3\big)(1-\sigma\theta_1)\big) = 0.$$

Thus, the associated eigenvalues are determined as $\lambda = d, \lambda = -(d+\kappa), \lambda = -d, \lambda = -e, \lambda = (d+\sigma)$,
or

$$\lambda^2 + (d+\rho-(\theta_3+d_3+d))\lambda + (\theta_3+d_3+d)(d+\rho) + \rho\theta_3 = 0. \tag{10}$$

Now to calculate for the remaining two eigenvalues of equation (10) we applied the local stability criteria described by Routh and Hurwitz and we verified that the necessary and sufficient conditions of the Routh and Hurwitz criteria holds whenever $\mathscr{R}_{ef} < 1$. Then, all the associated eigenvalues have negative real part whenever $\mathscr{R}_{ef} < 1$ and hence the HIV/AIDS and varicella-zoster co-infection model (4) disease-free equilibrium point has a local asymptotic stability property (is locally asymptotically stable) whenever $\mathscr{R}_{ef} < 1$ like similar approach used in Refs. [16,22]. Furthermore, the numerical simulation results verified that the HIV/AIDS and varicella-zoster co-infection model (4) disease-free equilibrium point is globally asymptotically stable whenever $\mathscr{R}_{ef} < 1$.

3.3.5. Existence and stability of endemic equilibrium point

In this sub-section, we need to calculate the HIV/AIDS and varicella-zoster co-infection model (4) endemic equilibrium point by considering the persistence of infections such that $\mathrm{H} \neq 0$, $\mathrm{P} \neq 0$, $\mathrm{A} \neq 0$ and $\mathrm{C} \neq 0$). Then, after some steps of the computations we have determined the required endemic equilibrium point for the co-infection model denoted by

$$E^*_{HZ} = (S^*, V^*, H^*, P^*, C^*, A^*, \mathrm{T}^*)$$

by substituting in incidence rates illustrated by

$$f_1{}^*(t) = \frac{\alpha_1}{N}(H^*(t) + \varepsilon_1 C^*(t)) \text{ and } f_2{}^*(t) = \frac{\alpha_2}{N}(P^*(t) + \varepsilon_2 C^*(t)).$$

Thus, the model (4) endemic equilibrium point is represented by

$$S^* = \frac{(1-P)\Delta}{(f_1{}^* + f_2{}^* + d)} + \frac{\kappa}{(f_1{}^* + f_2{}^* + d)}\left(\frac{p\Delta}{(\kappa+\mathrm{d})}\right), V^* = \frac{p\Delta}{(\kappa+\mathrm{d})},$$

$$\mathrm{H}^* = \left(\frac{1}{(\delta_1 f_1{}^* + \theta_2 + d_2 + \mathrm{d}) - (1-\sigma)\varphi}\right)\left(\frac{(1-p)\Delta f_1}{(f_1{}^* + f_2{}^* + d)} + \frac{\kappa f_1}{(f_1 + f_2{}^* + d)}\left(\frac{f_1 p\Delta}{(\kappa+d)}\right)\right),$$

$$\mathrm{P}^* = \left(\frac{(p-1)\Delta f_1{}^*}{(f_1 + f_2 + d)} - \frac{\kappa f_2{}^*}{(f_1 + f_2 + d)}\left(\frac{p\Delta}{(\kappa+\mathrm{d})}\right)\right)\left(\frac{(\sigma+\mu)}{\sigma\theta_1 - (\sigma+\mathrm{d})(\delta_2 f_2{}^* + \theta_1 + d_1 + \mathrm{d})}\right),$$

$$A^* = \frac{\theta_2 H^* + \theta_3 C^*}{(\rho+d)}, C^* = \frac{\delta_1 f_2 H^* + \delta_2 f_1 P^* + \rho A^*}{(\theta_3 + d_3 + \mathrm{d})},$$

and

$$\mathrm{T}^{*}=\left(\frac{\theta_1}{(\sigma+d)}\right)\left(\frac{(p-1)\Delta f_2^{*}}{(f_1+f_2+\mu)}-\frac{\kappa f_1^{*}}{(f_1+f_2+\mu)}\left(\frac{p\Delta}{(\kappa+\mathrm{d})}\right)\right)\left(\frac{(\sigma+\mathrm{d})}{\sigma\theta_1-(\sigma+\mathrm{d})(bf_1^{*}+\theta_1+d_1+\mathrm{d})}\right).$$

4. Construction of the optimal control problem and its qualitative analysis

In this part, our main objective is to analyze and solve the Optimal Control Problem to minimize the number of individuals co-infected with HIV/AIDS and varicella-zoster, while also aiming to reduce incurred costs. We have incorporated time-dependent control strategies into the co-infection model (4) to significantly manage the HIV/AIDS and varicella co-infection spreading dynamics in the community and to investigate various strategies for controlling spreading. By applying optimal control strategies in the constructed model (4), we aim to identify the most important intervention strategies to mitigate the spread of the HIV/AIDS and varicella co-infection spreading within a specified time frame. The intervention strategies considered for minimizing and eliminating the HIV/AIDS and varicella co-infection spreading include:

(a) Protection strategies: Implementing measures to prevent individuals from acquiring infection.
(b) Treatment strategies: Developing approaches to treat individuals already infected with HIV/AIDS and varicella-zoster.

Now, let's outline the particular control actions we implement for each of the two intervention strategies. In this part, we'll revise and assess the optimal control problem for the HIV/AIDS and varicella co-infection model (4) to investigate the most important control strategy for reducing the number of individuals with HIV/AIDS, varicella-zoster and both infections combined, all while minimizing the total intervention costs. Here the main aim is determining the optimal control values represented by $u^{*}=\left(u_1^{*},u_2^{*},u_3^{*},u_4^{*},u_5^{*}\right)$ for the control functions described by $u=(u_1,u_2,u_3,u_4,u_5)$ in order that the trajectories $S^{*},V^{*},H^{*},P^{*},C^{*},A^{*},T^{*}$ of the dynamical system (4) solutions at the interval of time illustrated by $\left[0,T_f\right]$ at the initial population illustrated by equation (5) and reducing the value of objective function. The time-dependent control functions we proposed incudes:

- The time-dependent function defined by $u_1(t)$ called the control function that interprets the attempts to protect HIV/AIDS infection in the community.
- The time-dependent function defined by $u_2(t)$ called the control function that interprets the attempts to protect varicella-zoster infected in the community.
- The time-dependent function defined by $u_3(t)$ called the control function that interprets the attempts to treat the HIV/AIDS infected in the community.
- The time-dependent function defined by $u_4(t)$ called the control function that interprets the attempts to treat of varicella-zoster infected in the community.
- The time-dependent function defined by $u_5(t)$ called the control function that interprets the attempts to treat the HIV/AIDS and varicella-zoster co-infected individuals in the community.

Therefore, implementing appropriate treatment and protection strategies for individuals co-infected with HIV/AIDS and varicella-zoster, as well as those singly infected with either virus, within a community is crucial for enhancing the recovery process and increasing the number of individuals who recover. This is subject to the condition that the control measures for each intervention strategy fall within the range of 0–1. After integrating the five control functions described earlier into the dynamic system (4), the resulting set of differential equations for the HIV/AIDS and varicella-zoster co-infection spreading model (4) can be expressed as follows:

$$\begin{aligned}
\frac{dS}{dt}&=(1-p)\Delta+\psi\ V-((1-u_1(t))f_1+(1-u_2(t))f_2+d)S,\\
\frac{d\mathrm{V}}{dt}&=p\Delta-(\psi+\mathrm{d})\mathrm{V},\\
\frac{d\mathrm{H}}{dt}&=(1-u_1(t))f_1S+(1-\psi)\varphi H-(\alpha_1f_1+u_3(t)\theta_2+d_2+\mathrm{d})\mathrm{H},\\
\frac{d\mathrm{P}}{dt}&=(1-u_2(t))f_2S+\sigma T-\left(\alpha_2f_1+u_4(t)\theta_1+d_1+\mathrm{d}\right)\mathrm{P},\\
\frac{d\mathrm{C}}{dt}&=\alpha_1f_2H+\alpha_2f_1P+\rho A-(\ u_5(t)\theta_3+d_3+d)\mathrm{C},\\
\frac{d\mathrm{A}}{dt}&=u_3(t)\theta_2\mathrm{H}+u_5(t)\theta_3\mathrm{C}-(\rho+d)\mathrm{A},
\end{aligned}\tag{11}$$

$$\frac{dT}{dt} = u_4(t)\theta_1 P - (\sigma + d)T,$$

subject to the initial population $S(0) = S^0 \geq 0$, $V(0) = V^0 \geq 0$, $H(0) = H^0 \geq 0$, $P(0) = P^0 \geq 0$, $C(0) = C^0 \geq 0$, $A(0) = A^0 \geq 0$, and $T(0) = T^0 \geq 0$.

Then we set the objective functional represented by

$$J(u_1, u_2, u_3, u_4, u_5) = \int_0^{T_f} \left(D_1 H + D_2 P + D_3 C + \frac{1}{2} \sum_{i=1}^{5} \psi_i u_i^2 \right) dt, \tag{12}$$

where T_f is the final time D_1, D_2 and D_3 are weight constants of the HIV infected, the Varicella-Zoster infected and HIV/AIDS and Varicella-Zoster co-infected individuals respectively while u_i for $i = 1, ..., 5,$ are weight constants for each individual control function. We choose a nonlinear cost on the controls based on the assumption that the costs take nonlinear form as applied in Refs. [14,19,25,30,37].

Let us state the main objective of the constructed optimal control problem for the co-infection model (4) as to investigate the optimal control measures illustrated by $u_1^*, u_2^*, u_3^*, u_4^*, u_5^*$ such that

$$J\left(u_1^*, u_2^*, u_3^*, u_4^*, u_5^*\right) = min\{J(u_1, u_2, u_3, u_4, u_5) : u_1, u_2, u_3, u_4, u_5 \in U\}, \tag{13}$$

where $U = \left\{ u_1(t), u_2(t), u_3(t), u_4(t), u_5(t) \in \mathbb{R}^5 \right\}$ such that $u_1(t), u_2(t), u_3(t), u_4(t), u_5(t)$ are Lebesgue measurable functions and $0 \leq u_1(t), u_2(t), u_3(t), u_4(t), u_5(t) \leq 1$ for $0 \leq t \leq T_f$ is the control set.

Theorem 3. Given $J(u_1, u_2, u_3, u_4, u_5)$ subject to the system equation (11), then there are optimal control measures $u^* = \left(u_1^*, u_2^*, u_3^*, u_4^*, u_5^*\right)$ and associated optimal solutions to the initial value problem (11)-(13) by $(S^*, V^*, H^*, P^*, C^*, A^*, T^*)$, that minimizes $J(u_1, u_2, u_3, u_4, u_5)$ over U.

Proof. To verify the following four basic conditions required for the set of admissible controls U we can use the Fleming and Rishel's theorem stated in 38.

C_1: The set of the co-infection model (4) variables to system (11)–(13) that correspond to the control functions in U is non-empty.

C_2: The set U called the control set is both closed and convex.

C_3: Every right hand side function of the control problem is continuous, is bounded above by a sum of the bounded control and the state, and can be represented a linear function of the control function $u = (u_1, u_2, u_3, u_4, u_5)$ where the coefficients are depend on time and the state variables.

C_4: The objective functional integrand that is given in equation (24) is convex.

The first required condition (C_1) can be verified by using the theorem described and proved by Picard-Lindelöf's. If the co-infection model optimal control problem solutions remain bounded, continuous, and adhere to Lipschitz conditions in the co-infection model state variables, a unique solution exists for each permissible control U. We have proved that the number of human population at a given time t is bounded like $0 \leq N(t) \leq \frac{\Lambda}{d}$ also every state variables of the model is bounded. The state variables of the model remain continuous and limited in range. Likewise, we can demonstrate that the partial derivatives concerning the state variables are bounded. This confirms that the model is Lipschitz regarding the state variables. This completes the verification that condition C_1 holds.

By applying definition stated in Refs. [39,40], the control set U is convex and closed this proved the required condition C_2. Condition C_3 is verified by observing the linear dependent conditions of the co-infection model optimal control problem equations on the control variables u_1, u_2, u_3, u_4, u_5.

Eventually, to justify the required condition C_4 use definition stated in Refs. [41,42] that says any function which is constant function or linear function or quadratic function is convex. Hence, since the integrand of the objective functional given by $L(x, u, t) = D_1 H + D_2 P + D_3 C + \frac{1}{2}\psi_1 u_1^2 + \frac{1}{2}\psi_2 u_2^2 + \frac{1}{2}\psi_3 u_3^2 + \frac{1}{2}\psi_4 u_4^2 + \frac{1}{2}\psi_5 u_5^2$ is a quadratic function which is convex function on U. To show the bound on $L(x, u, t)$ use definition of the control function U as: then we have $\frac{1}{2}\psi_5 u_5^2 \leq \frac{1}{2}\psi_5$ since $0 \leq u_5 \leq 1$ and hence

$$\frac{1}{2}\omega\psi_5 u_5^2 - \frac{1}{2}\psi_5 \leq 0.$$

$$\Longrightarrow L(x, u, t) = D_1 H + D_2 P + D_3 C + \frac{1}{2}\psi_1 u_1^2 + \frac{1}{2}\psi_2 u_2^2 + \frac{1}{2}\psi_3 u_3^2 + \frac{1}{2}\psi_4 u_4^2 + \frac{1}{2}\psi_5 u_5^2 \geq \frac{1}{2}\psi_1 u_1^2 + \frac{1}{2}\psi_2 u_2^2 + \frac{1}{2}\psi_3 u_3^2 + \frac{1}{2}\psi_4 u_4^2 + \frac{1}{2}\psi_5 u_5^2 - \frac{1}{2}\psi_5.$$

$$\Longrightarrow L(x, u, t) \geq \min\left\{\frac{1}{2}\psi_1, \frac{1}{2}\psi_2, \frac{1}{2}\psi_3, \frac{1}{2}\psi_4, \frac{1}{2}\psi_5\right\}\left(u_1^2 + u_2^2 + u_3^2 + u_4^2 + u_5^2\right) - \frac{1}{2}\psi_5.$$

$$\Longrightarrow L(x, u, t) \geq \min\left\{\frac{1}{2}\psi_1, \frac{1}{2}\psi_2, \frac{1}{2}\psi_3, \frac{1}{2}\psi_4, \frac{1}{2}\psi_5\right\}\left(|(u_1, u_2, u_3, u_4, u_5)|^2\right) - \frac{1}{2}\psi_5.$$

$$\Longrightarrow \mathrm{L}(\mathrm{x},\mathrm{u},\mathrm{t}) \geq M_1|u|^{\beta} - M_2, \text{where } M_1 = \min\left\{\frac{1}{2}\psi_1, \frac{1}{2}\psi_2, \frac{1}{2}\psi_3, \frac{1}{2}\psi_4, \frac{1}{2}\psi_5\right\}, M_2 = \frac{1}{2}\psi_5,$$

$u = (u_1, u_2, u_3, u_4, u_5),$ and $\beta = 2$. This completes the proved of Theorem 3 above.

According to the Pontryagin's maximum principle criteria that are necessary for an optimal solution holds we convert system (11)–(14) in to a required problem that minimizes the Hamiltonian function denoted by $\mathscr{H}$ at the controls u_1, u_2, u_3, u_4, u_5 including the state equation and the adjoint property.

The corresponding Hamiltonian function is represented by the function

$$\begin{aligned}
\mathscr{H} &= D_1 H + D_2 P + D_3 C + \frac{1}{2}\psi_1 u_1^2 + \frac{1}{2}\psi_2 u_2^2 + \frac{1}{2}\psi_3 u_3^2 + \frac{1}{2}\psi_4 u_4^2 + \frac{1}{2}\psi_5 u_5^2 \\
&+\lambda_1((1-p)\Delta + \psi\, V - ((1-u_1(t))f_1 + (1-u_2(t))f_2 + d)S) \\
&+\lambda_2(p\Delta - (\psi + \mathrm{d})\mathrm{V}) \\
&+\lambda_3((1-u_1(t))f_1 S + (1-\psi)\varphi H - (\alpha_1 f_1 + u_3(t)\theta_2 + d_2 + \mathrm{d})\mathrm{H}) \\
&+\lambda_4\big((1-u_2(t))f_2 S + \sigma T - \big(\alpha_2 f_1 + u_4(t)\theta_1 + d_1 + \mathrm{d}\big)\mathrm{P}\big) \\
&+\lambda_5(\alpha_1 f_2 H + \alpha_2 f_1 P + \rho A - (\, u_5(t)\theta_3 + d_3 + d)\mathrm{C}) \\
&+\lambda_6\big(u_3(t)\theta_2 \mathrm{H} + u_5(t)\theta_3 \mathrm{C} - (\rho + d)\mathrm{A}\big) \\
&+\lambda_7(u_4(t)\theta_1 P - (\sigma + d)T),
\end{aligned} \tag{14}$$

where λ_i, $i = 1, \ldots, 7$ are the adjoint variables.

Theorem 4. *For an optimal control set u_1, u_2, u_3, u_4, u_5 that minimizes J over U, there is an adjoint variables, $\lambda_1, \ldots, \lambda_7$ such that:*

$$\frac{d\lambda_1}{dt} = (\lambda_1 - \lambda_3)(1-u_1(t))\left(\frac{\alpha_1(H(t)+\varepsilon_1 C(t))N - \alpha_1(H(t)+\varepsilon_1 C(t))S}{N^2}\right) + (\lambda_1$$
$$-\lambda_4)(1-u_2(t))\left(\frac{\alpha_2(P(t)+\varepsilon_2 C(t))N - \alpha_2(P(t)+\varepsilon_2 C(t))S}{N^2}\right) + \lambda_1 d + (\lambda_5 - \lambda_4)\delta_2\alpha_1\left(\frac{H(t)+\varepsilon_1 C(t)}{N^2}\right)\mathrm{P}$$
$$+(\lambda_5 - \lambda_3)\delta_1\alpha_2\left(\frac{P(t)+\varepsilon_2 C(t)}{N^2}\right)\mathrm{H} + \lambda_1 d,$$

$$\frac{d\lambda_2}{dt} = (\lambda_2 - \lambda_1)\psi + \lambda_2 \mathrm{d},$$

$$\frac{d\lambda_3}{dt} = (\lambda_1 - \lambda_3)(1-u_1(t))\left(\frac{\alpha_1 SN - \alpha_1(H(t)+\varepsilon_1 C(t))S}{N^2}\right) + (\lambda_4 - \lambda_1)\alpha_2(1-u_2(t))\left(\frac{(P(t)+\varepsilon_2 C(t))S}{N^2}\right) +$$
$$+(\lambda_4 - \lambda_5)\alpha_1\delta_2\left(\frac{N - (H(t)+\varepsilon_1 C(t))P}{N^2}\right) + (2\lambda_3 - \lambda_5)\alpha_2\delta_1\left(\frac{(P(t)+\varepsilon_2 C(t))N - (P(t)+\varepsilon_2 C(t))H}{N^2}\right) - + (\lambda_3 - \lambda_6)u_3(t)\theta_2 + \lambda_3(d_2 + \mathrm{d}$$
$$-(1-\psi)\varphi) - D_1,$$

$$\begin{aligned}
\frac{d\lambda_4}{dt} &= (\lambda_3 - \lambda_1)(1-u_1(t))\alpha_1\frac{(H(t)+\varepsilon_1 C(t))S}{N^2} + (\lambda_1 - \lambda_4)(1-u_2(t))\alpha_2\left(\frac{NS - (P(t)+\varepsilon_2 C(t))S}{N^2}\right) + (\lambda_4 - \lambda_5)\delta_2\alpha_1 \\
&\left(\frac{(H(t)+\varepsilon_1 C(t))N - (P(t)+\varepsilon_1 C(t))P}{N^2}\right) + (\lambda_3 - \lambda_5)\delta_1\alpha_2\left(\frac{NH - (P(t)+\varepsilon_2 C(t))H}{N^2}\right) + (\lambda_4 - \lambda_7)u_4(t)\theta_1 + \lambda_4(d_1 + \mathrm{d}) - D_2,
\end{aligned}$$

$$\begin{aligned}
\frac{d\lambda_5}{dt} &= (\lambda_1 - \lambda_3)(1-u_1(t))\alpha_1\left(\frac{\varepsilon_1 NS - (H(t)+\varepsilon_1 C(t))S}{N^2}\right) + (\lambda_1 - \lambda_4)(1-u_2(t))\alpha_2\left(\frac{\varepsilon_2 NS - (P(t)+\varepsilon_2 C(t))S}{N^2}\right) + (\lambda_4 - \lambda_5)\delta_2\alpha_1 \\
&\left(\frac{\varepsilon_1 NP - (H(t)+\varepsilon_1 C(t))P}{N^2}\right) + (\lambda_3 - \lambda_5)\delta_1\alpha_2\left(\frac{\varepsilon_2 NH - (P(t)+\varepsilon_2 C(t))H}{N^2}\right) + (\lambda_5 - \lambda_6)\, u_5(t)\theta_3 + \lambda_5\,(d_3 + d) - D_3,
\end{aligned} \tag{15}$$

$$\frac{d\lambda_6}{dt} = (\lambda_3 - \lambda_1)(1-u_1(t))\alpha_1\frac{(H(t)+\varepsilon_1 C(t))S}{N^2} + (\lambda_4 - \lambda_1)(1-u_2(t))\alpha_2\frac{(P(t)+\varepsilon_2 C(t))S}{N^2} + (\lambda_5 - \lambda_4)\delta_2\alpha_1\frac{(H(t)+\varepsilon_1 C(t))P}{N^2} +$$
$$(\lambda_5 - \lambda_3)\delta_1\alpha_2\frac{(P(t)+\varepsilon_2 C(t))H}{N^2} + (\lambda_6 - \lambda_5)\rho + \lambda_6 d,$$

$$\Big((\lambda_3-\lambda_1)(1-u_1(t))\alpha_1\frac{(H(t)+\varepsilon_1C(t))S}{N^2}+(\lambda_4-\lambda_1)(1-u_2(t))\alpha_2\frac{(P(t)+\varepsilon_2C(t))S}{N^2}+(\lambda_5-\lambda_4)\delta_2\alpha_1\frac{(H(t)+\varepsilon_1C(t))P}{N^2}+$$
$$(\lambda_5-\lambda_3)\delta_1\alpha_2\frac{(P(t)+\varepsilon_2C(t))H}{N^2}+(\lambda_7-\lambda_4)\sigma+\lambda_7 d,(\lambda_3-\lambda_1)(1-u_1(t))\alpha_1\frac{(H(t)+\varepsilon_1C(t))S}{N^2}$$
$$+(\lambda_4-\lambda_1)(1-u_2(t))\alpha_2\frac{(P(t)+\varepsilon_2C(t))S}{N^2}+(\lambda_5-\lambda_4)\delta_2\alpha_1\frac{(H(t)+\varepsilon_1C(t))P}{N^2}+(\lambda_5-\lambda_3)\delta_1\alpha_2\frac{(P(t)+\varepsilon_2C(t))H}{N^2}+(\lambda_7-\lambda_4)\sigma+\lambda_7 d,$$

with the final conditions $\lambda_i(T_f)=0$, for $i=1,\ldots,7$.

Proof. Let us use the necessary and sufficient conditions stated as

$$\begin{aligned}
&\frac{d\lambda_1}{dt}=-\frac{\partial\mathscr{H}}{\partial S},\frac{d\lambda_4}{dt}=-\frac{\partial\mathscr{H}}{\partial P},\\
&\frac{d\lambda_2}{dt}=-\frac{\partial\mathscr{H}}{\partial V},\frac{d\lambda_5}{dt}=-\frac{\partial\mathscr{H}}{\partial C},\\
&\frac{d\lambda_3}{dt}=-\frac{\partial\mathscr{H}}{\partial H},\frac{d\lambda_6}{dt}=-\frac{\partial\mathscr{H}}{\partial A},\text{and }\frac{d\lambda_7}{dt}=-\frac{\partial\mathscr{H}}{\partial T}.
\end{aligned}\tag{16}$$

Then solving the results of (16) the full expression of the adjoint functions $\frac{d\lambda_i}{dt}$ for $i=1,2,3,4,5,6,7$ of the optimal control system (11) based on (14) and (15) are given by system (15). This proved the theorem.

The criteria that verifies optimality: The optimality criteria we have explored, guided by Pontryagin's Maximum Principle, focus on minimizing the Hamiltonian H with respect to the control functions u_1, u_2, u_3, u_4 and u_5. Considering the convexity of the cost function, if the optimal control resides within the interior region, we must adhere to the following fundamental necessary and sufficient optimality conditions for the optimal control problem (11):

$$\frac{\partial\mathscr{H}}{\partial u_1^*}=0,\frac{\partial\mathscr{H}}{\partial u_2^*}=0,\frac{\partial\mathscr{H}}{\partial u_3^*}=0,\frac{\partial\mathscr{H}}{\partial u_4^*}=0,\text{and }\frac{\partial\mathscr{H}}{\partial u_5^*}=0.\tag{17}$$

After solving and simplifying the results we have determined the final optimal control strategies results given by:

$$u_1^*=\max\{0,\min\{1,\frac{(\lambda_3-\lambda_1)f_1S}{\psi_1}\}\},$$

$$u_2^*=\max\{0,\min\{1,\frac{(\lambda_4-\lambda_1)f_2S}{\psi_2}\}\},$$

$$u_3^*=\max\{0,\min\{1,\frac{(\lambda_3-\lambda_6)\theta_2H}{\psi_3}\}\},$$

$$u_4^*=\max\{0,\min\{1,\frac{(\lambda_4-\lambda_7)\theta_1P}{\psi_4}\}\},$$

$$u_5^*=\max\{0,\min\{1,\frac{(\lambda_5-\lambda_6)\theta_3PC}{\psi_5}\}\}.$$

Theorem 5. *For any $t\in[0,T_f]$, the bounded solutions to the optimality system are unique. We can refer* [43], *for the proof of the theorem.*

5. Investigation of parameters sensitivity and numerical analysis

5.1. Investigation of the parameters sensitivity

Now we need to investigate the significance of each model parameter that affects the spread of the disease. Using criteria similar to those described in Ref. [42], we conducted sensitivity analyses to understand how different parameters affect the effective reproduction ratio of the HIV/AIDS and varicella-zoster co-infection dynamical system (4). These analyses help us identify which parameters have the greatest influence on the spread of the co-infection disease. By pinpointing the most sensitive parameters those with higher sensitivity indices we gain valuable insights into which factors play the most significant role in driving the spread of the disease. Specifically, our sensitivity analyses focused on parameters $\mathscr{R}_1$ and $\mathscr{R}_2$, allowing us to better understand their impact on the spread of the co-infection.

(1) $SI(\kappa)=\frac{\kappa(d-d(1-p))}{(d+\kappa)(\kappa+d(1-p))}$.

(2) $SI(\Delta)=1$.

(3) $SI(\varphi) = -\frac{(\sigma-1)\varphi}{d-\varphi+\sigma\varphi+d_2+\theta_2}$.

(4) $SI(\alpha_1) = \frac{\kappa+d[1-p]}{(d+\kappa)(d-\varphi+\sigma\varphi+d_2+\theta_2)}\left(\frac{\alpha_1}{\mathscr{R}_1}\right) = 1$.

(5) $SI(\sigma) = -\frac{\sigma\varphi}{d-\varphi+\sigma\varphi+d_2+\theta_2}$.

(6) $SI(\alpha_2) = \frac{\kappa+d[1-p]}{(d+\kappa)(d+d_1+\theta_1)}\left(\frac{\alpha_2}{\mathscr{R}_2}\right) = 1$.

The model parameters sensitivity investigation results by using the parameter values described by Table 2 and considering the co-infection model effective reproduction number $\mathscr{R}_{ef}$ as a response function illustrated by Fig. 2 reveals that the top three most sensitive parameters are the recruitment rate, the spreading rate, and the zoster vaccination coverage portion. These parameters emerge as influential factors, shaping the dynamics of HIV/AIDS and varicella-zoster co-infection disease spreading within the population. These findings underscore the importance of considering these variables in understanding and addressing the spread of HIV/AIDS and varicella-zoster infections.

Table 2
Parameter Values used in the Co-infection Model.

Parameter	Values	References
d	0.1	[21]
Δ	100	[39]
p	0.8	Estimated from [24]
κ	0.35	Estimated
δ_1	1	Estimated
δ_2	1	Estimated
d_1	0.32	Estimated from [24]
d_2	0.29	Assumed
d_3	0.3	Assumed
$\boldsymbol{\sigma}$	0.65	Estimated from [24]
ρ	0.32	Estimated
α_1	2.5	Estimated from [13]
α_2	3.5	[24]
θ_1	0.87	Estimated from [24]
θ_2	0.45	Estimated from [13]
θ_3	0.53	Assumed
ψ	0.35	Estimated
$\boldsymbol{\varphi}$	0.6	Estimated

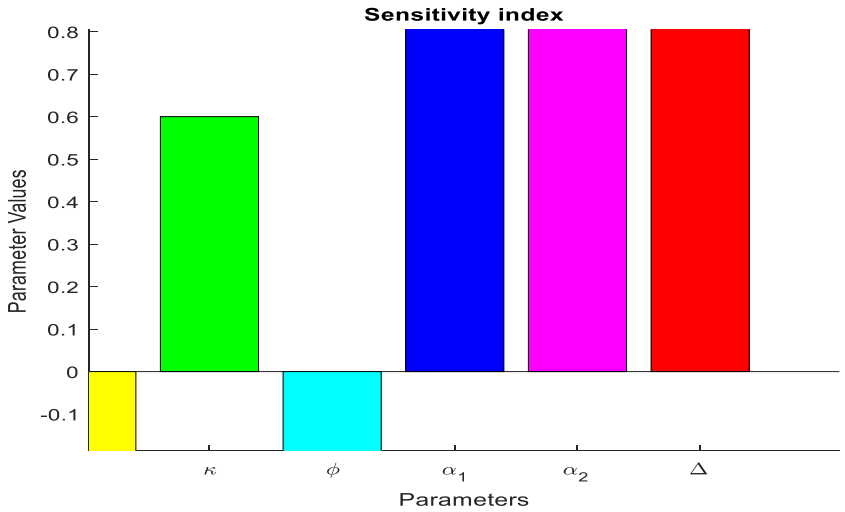

Fig. 2. The diagram that reveals the HIV/AIDs and varicella-zoster co-infection model sensitivity analyses.

5.2. Simulations for the of HIV/AIDS and zoster co-infection model

The HIV/AIDS and varicella-zoster dynamical system (4) is highly non-linear and complex and hence investigating every analytical solution for this dynamical system is more complicated and extremely difficult. To examine the solutions in the case of such complexities, it becomes essential to perform numerical simulation of the dynamical system particularly important when validating the predictions of a mathematical model regarding the dynamics of HIV/AIDS and varicella-zoster co-infection. In this sub-section, we have applied the Runge-Kutta fourth order numerical forward scheme method with MATLAB and performed simulations using parameter values described in Table 2 to investigate the behavior of co-infection model (4) solutions over time, and then comparing the simulation results as discussed in Ref. [16]. In this part of the study, the aim is to investigate the impacts of various characteristics (parameters) related to HIV/AIDS and zoster co-infection, such as treatment rate, portion of vaccination, and vaccination decay rate.

The numerical simulation graph presented by Fig. 3 depicts the HIV/AIDS and Varicella-Zoster co-infection model (4) disease-free equilibrium point local asymptotic stability whenever its associated effective reproduction number is below one $(\mathscr{R}_{ef} < 1)$. This plot also highlights the biological significance of the spread and expansion of HIV/AIDS and Varicella-Zoster co-infection within a population restricted to a particular area, demonstrating that the infection will dies out if this condition is met.

The numerical simulation diagram presented by Fig. 4 above reveals the result that the solutions of the HIV/AIDS and Varizola-

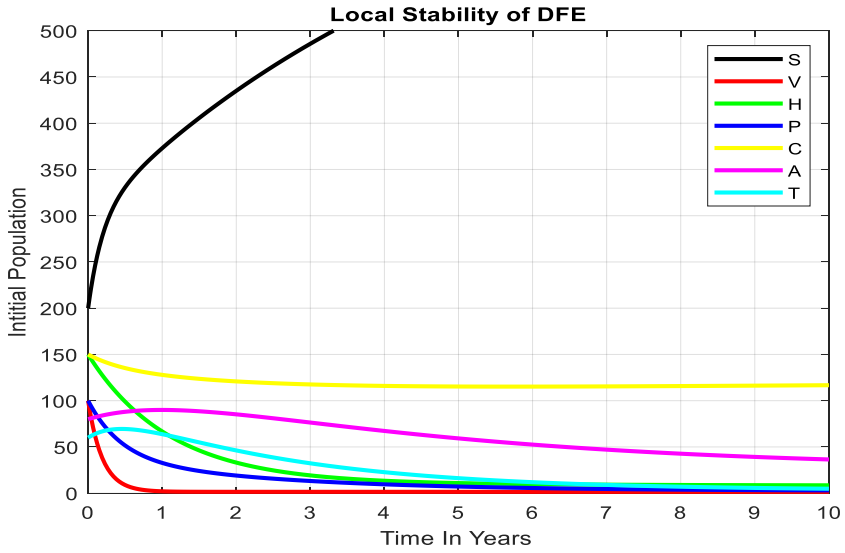

Fig. 3. Behaviors of the HIV/AIDS and Varicella-Zoster co-infection model (4) solutions whenever $\mathscr{R}_{ef} < 1$..

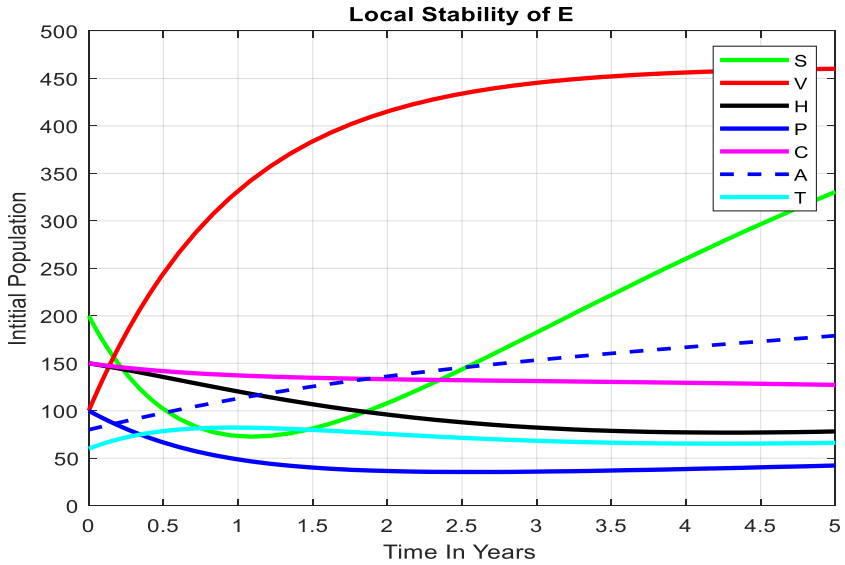

Fig. 4. The behavior of the HIV/AIDS and Varicella-Zoster co-infection model (4) solutions whenever $\mathscr{R}_{ef} > 1$..

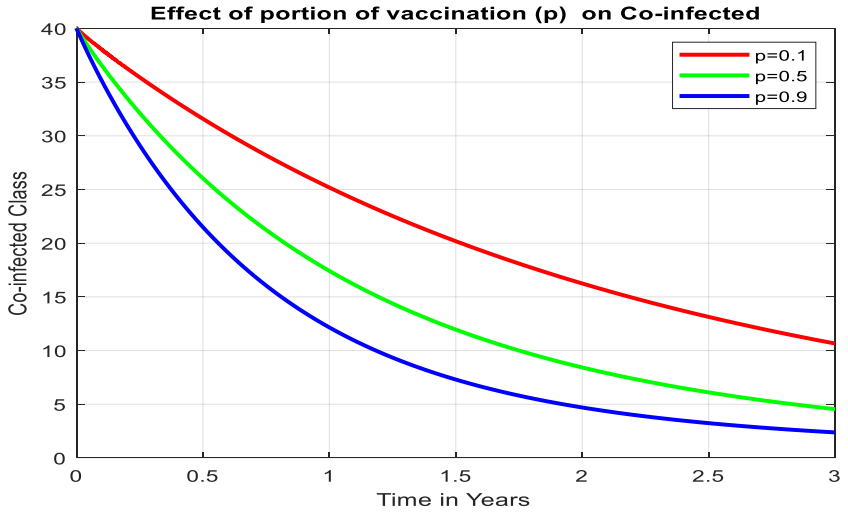

Fig. 5. Simulation to reveals the impact of portion of zoster vaccination (p) on the HIV/AIDS and Varicella-Zoster co-infected individuals.

Zoster co-infection dynamical system (4) will converge towards its endemic equilibrium point whenever $\mathscr{R}_{ef} > 1$. From a biological standpoint, this suggests that the HIV/AIDS and Varizola-Zoster co-infection disease spreads uniformly within the community.

The simulation results depicted in Fig. 5 indicates that as the portion of vaccination for zoster disease rises, there is a decline in the number of individuals co-infected with HIV/AIDS and Varicella-Zoster. Therefore, increasing the portion of vaccination is the best control measure to mitigate the co-infection disease spreading in the population. Thus, higher portion of vaccination can alleviate potential complications resulting from the co-infection of HIV/AIDS and Varicella-Zoster.

The simulation fraph described by Fig. 6 invesigates and reveals that as the treatment rate for HIV/AIDS and Varicella-Zoster co-infected individuals increases implies the number of zoster-infected individuals decreases. Consequently, treating the HIV/AIDS and Varicella-Zoster co-infected individuals represents another fundamental approach to minimize and control the prevalence of these diseases in the population under consideration.

Based on the simulation results described by Fig. 7, we can observe the influence of the vaccination portion (p) on the co-infection model effective reproduction number $\mathscr{R}_{ef}$. The diagram (Fig. 7) reveals that as the value of the portion p increases, both the reproduction numbers $\mathscr{R}_1$ *and* $\mathscr{R}_2$ decrease, leading to a decline in their maximum value as well. Moreover, the value of $\mathscr{R} = max\{\mathscr{R}_1, \mathscr{R}_2\}$ less than one whenever the value of the portion p more than 0.3.

The simulation result re-presented by Fig. 8 explore how the diseases spreading rates described by $\{\alpha_1$ and $\alpha_2\}$ affect the overall spread of HIV/AIDS and varicella-zoster co-infection in the population. It's clear that as the values of α_1, and α_1 increase then the values of both $\mathscr{R}_1$ and $\mathscr{R}_2$ rise as well. To keep the spread of the disease under control the value of the co-infection model (4)

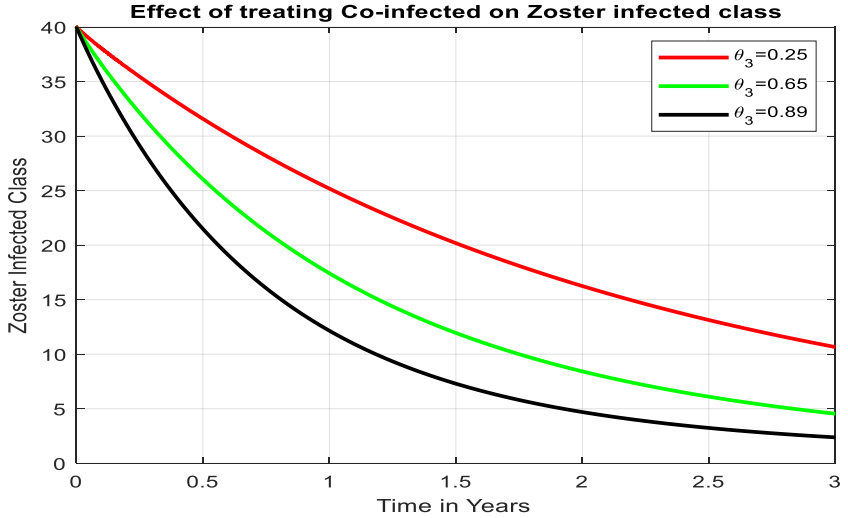

Fig. 6. Simulation to reveals the impact of treatment of the HIV/AIDS and Varicella-Zoster co-infection treatment (θ_3) on the varicella-zoster infected individuals.

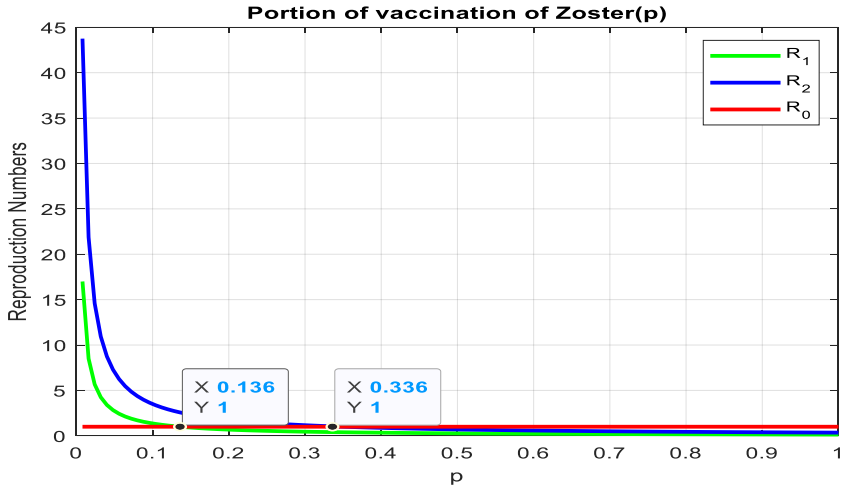

Fig. 7. Simulation results to reveal the impact of portion of vaccination (p) on various reproduction numbers consideration for the co-infection model (4).

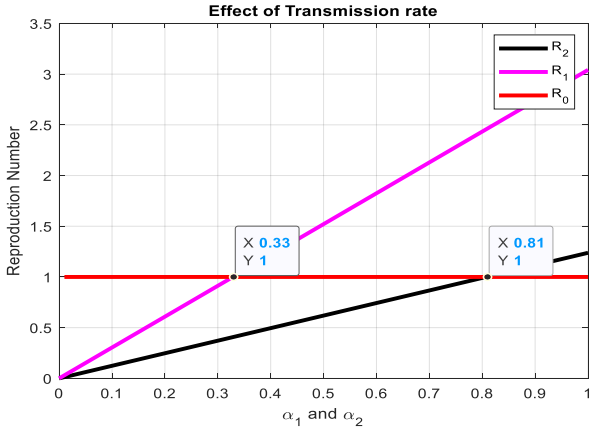

Fig. 8. Simulation result that reveals the impact of the spreading rates (α_1, α_1) on various reproduction numbers of the co-infection model (4).

represented by $\mathscr{R}_{ef} = max\{\mathscr{R}_1, \mathscr{R}_2\}$, should be less than 0.33. Therefore, it is fundamental on focusing to lower the diseases spreading rates for both HIV/AIDS and Zoster diseases.

The simulation graph represented Fig. 9 explains the possible impact of Zoster vaccination waning rate (κ) on the HIV/AIDS and Varicella-Zoster co-infection model (4) effective reproduction number described $\mathscr{R}_{ef} = max\{\mathscr{R}_1, \mathscr{R}_2\}$. The result reveals that the values of both $\mathscr{R}_1$ and $\mathscr{R}_2$ grow whenever the value of vaccination waning rate (κ) rises. One can concluded that the whenever the value of vaccination waning rate (κ) is smaller than 0.81, the minimum value of the HIV/AIDS and Varicella-Zoster co-infection dynamical system (4) effective reproduction number $\mathscr{R}_{ef} = max\{\mathscr{R}_1, \mathscr{R}_2\} = max\{1.78, 2.76\} = 2.76$ is attained. The impact of zoster vaccination in preventing the HIV/AIDS and Varicella-Zoster co-infection spreading in the community should be carefully observed and made decisions by the public health stakeholders.

5.3. Numerical simulation of the optimal control problem

Using the same numerical methods used in the sub-section 5.2, in this sub-section, we carried out numerical simulations for the constructed optimal control problem to investigate the best control strategies over time to achieve specified objectives with the associated constraints. The process we carried out in this sub-section also gives insights into the control problem system dynamics, the optimizing performance, and assessing the robustness of the proposed control strategies across various applications. Incorporating optimal control theory in the proposed study is highly significant, as it introduces five control strategies aimed at managing the spreading dynamics of HIV/AIDS and varicella-zoster co-infection in the population. The proposed time-dependent control strategies encompass preventing of HIV/AIDS and zoster infections, enhancing recovery from each infection, and providing treatment for the HIV/AIDS and varicella-zoster co-infected individuals. This sub-section also emphasizes the critical importance of the five proposed control strategies, both collectively and individually, highlighting their role in shaping the best effective approaches to address the

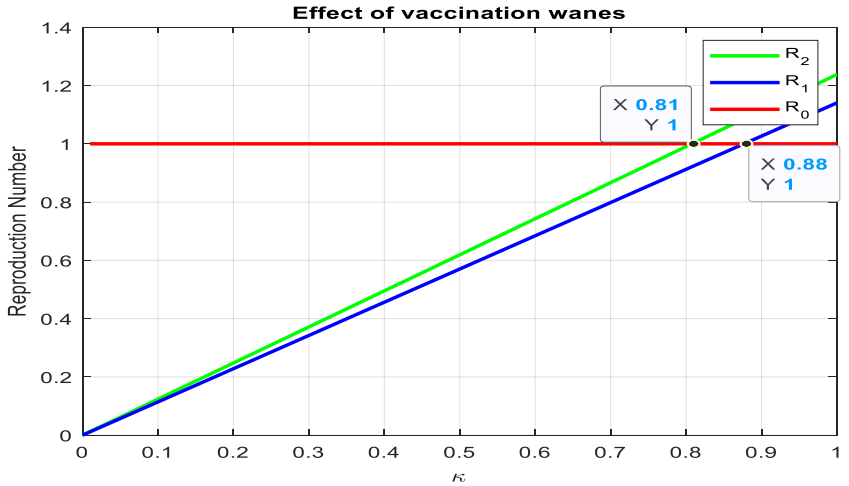

Fig. 9. Simulation result to reveals the impact of the Zoster vaccination waning rate (κ) on various reproduction numbers of the co-infection model (4).

complexities of HIV/AIDS and varicella-zoster co-infection spreading dynamics in the community. Performing the numerical analysis computations enables researchers to explore the behavior of these control strategies in various scenarios, providing valuable insights that contribute to the development of best effective intervention strategies for managing the HIV/AIDS and varicella-zoster co-infection.

Simulation results represented by Figs. 10 and 11 reveal how the particular control strategy influences the spreading dynamics of HIV/AIDS-infected individuals. The result collected from Fig. 10 indicated that the implementation of the control strategy u_1 leads to a sharp decrease in the number of HIV/AIDS-infected individuals compared to the scenario where this approach is not applied. Similarly, the result collected from Fig. 11 demonstrates the impact of the control strategy u_2 on the same population, showing a significant reduction in the number of infected individuals compared to when this control is absent. These noticeable declines highlight the effectiveness of these control measures in curbing the spread of HIV/AIDS infection, underscoring their critical role in public health interventions.

The impacts of the two control measures (u_3, u_3) on the HIV/AIDS infection in biological aspects can be investigated from simulations results represented by Figs. 12 and 13. The finding collected from Fig. 12 reveals the significance of u_3 on the HIV/AIDS infection spreading dynamics that means it depicts that a rapid decline in the HIV/AIDS infected population. Similarly the result collected from the simulation finding described by Fig. 13 shows the impact of u_4 on the HIV/AIDS infection spreading dynamics, having similar decline approach. The findings discussed in this part highlight the biological efficacy of these control strategies in reducing the spread of HIV/AIDS in the community, underscoring their crucial role in shaping the best effective intervention strategies

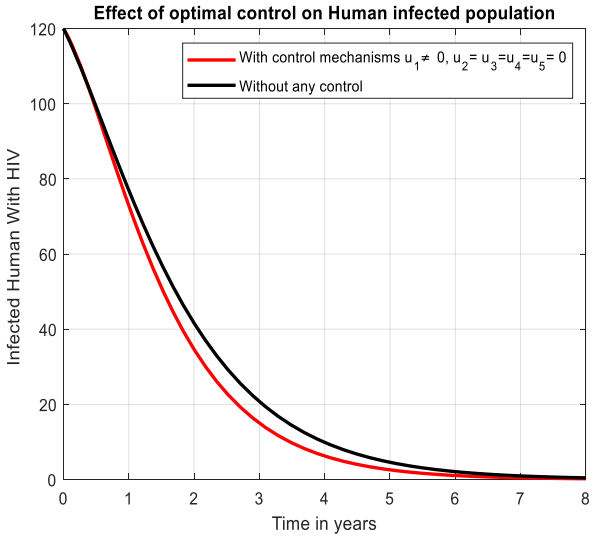

Fig. 10. Simulation to reveals impact of control strategy u_1 on HIV/AIDS infection.

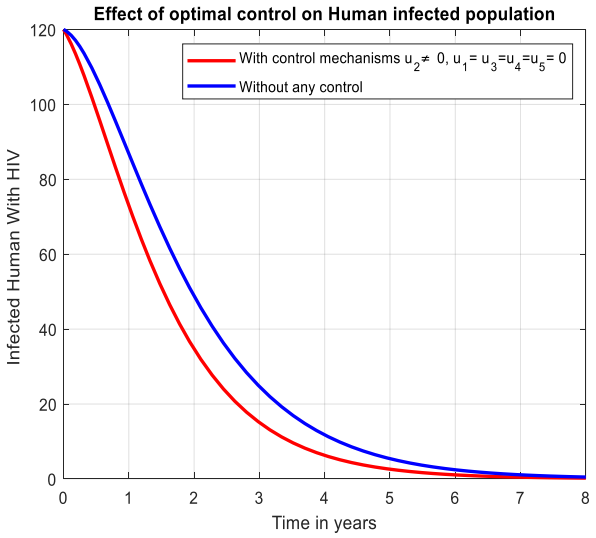

Fig. 11. Simulation to reveals impact of control strategy $\boldsymbol{u_2}$ on HIV/AIDS infection.

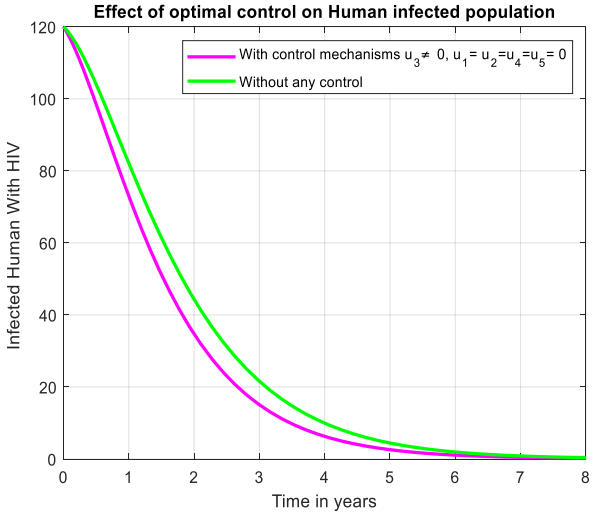

Fig. 12. Simulation to reveals impact of control strategy u_3 on HIV/AIDS infection.

and mitigating the impact of the HIV/AIDS infection in the community. The charts shown in Figs. 12 and 13 above show the biological impact of the two control strategies denoted by (u_3 and u_4) on HIV/AIDS-infected individuals. Fig. 12 demonstrates the impact of the control strategy u_3 on HIV/AIDS infection, showing a significant decrease in the HIV/AIDS-infected population. Similarly, Fig. 13 examines the impact of the control strategy u_4 on HIV/AIDS infection, revealing a comparable decline. These results emphasize the biological effectiveness of these controls in curtailing the spread of HIV, highlighting their pivotal role in shaping the best effective intervention strategies and mitigating the impact of HIV/AIDS infection in the community.

The simulation results in this part are represented by Figs. 14 and 15 and investigated the impacts of the control function u_5 on the HIV/AIDS-infection and the crucial impact of the aggregate control measures u_1, u_2, u_3, u_4 and u_5 on the HIV/AIDS-infected population respectively. Unlike situations where these control strategies are not used, the result collected from graph shows a sharp decrease in the number of HIV/AIDS-infected individuals. This highlights the combined and powerful impact of the comprehensive intervention strategy. The visual representation underscores the collective effectiveness of the control measures for reducing the spread of HIV/AIDS, emphasizing the crucial significance of a multifaceted approach in managing and alleviating the infection's impact on the population.

The findings collected from the results represented by Figs. 16 and 17 revealed the impact of implementing the control measure u_3 on the varicella-zoster infection, showing a reduction of the zoster infected individuals and examined the combined impact of the two control measures u_3 and u_4 , on the same class show a greater decline respectively. From a biological perspective, the findings emphasize that the significance of understanding how the control strategies interact; offering valuable insights for devising optimized intervention strategies against varicella-zoster infections in the community.

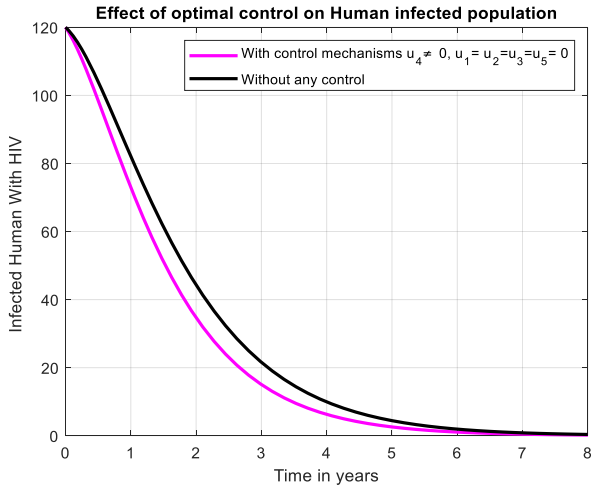

Fig. 13. Simulation to reveals impact of control strategy u_4 on HIV/AIDS infection.

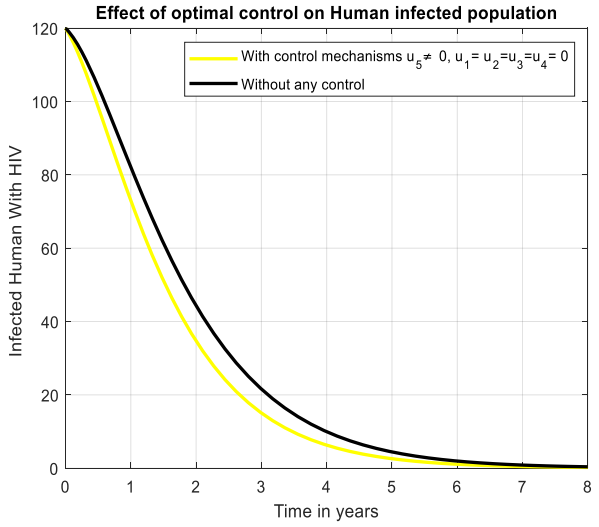

Fig. 14. Simulation result to reveals the impact of u_5 on the HIV/AIDS infection.

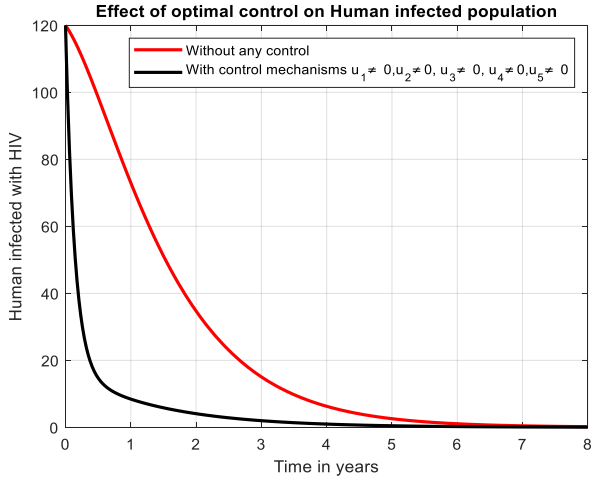

Fig. 15. Simulation result to reveals the impacts of $\boldsymbol{u_1}$, $\boldsymbol{u_2}$, $\boldsymbol{u_3}$, $\boldsymbol{u_4}$ and $\boldsymbol{u_5}$ on the HIV/AIDS infection.

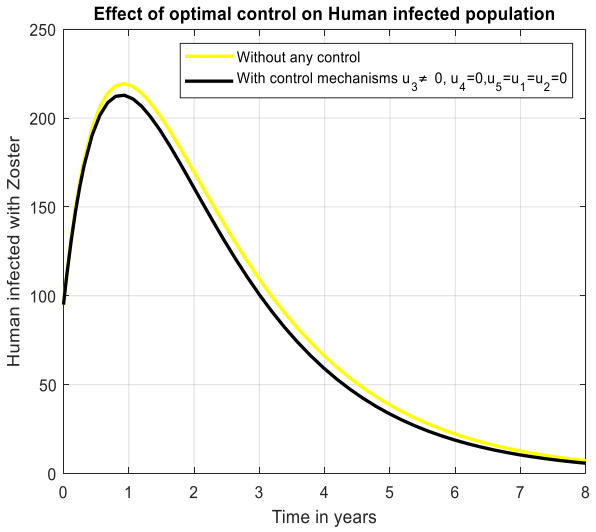

Fig. 16. Simulation to reveals the impact of the control measure u_3 on the zoster infection.

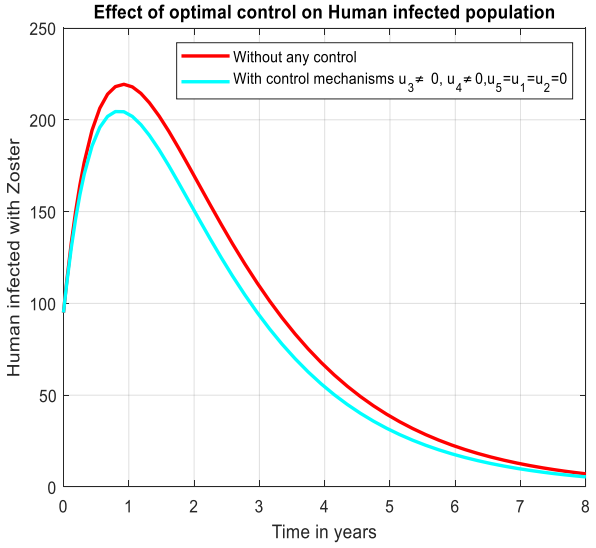

Fig. 17. Simulation to reveals the impact of the control measures u_3 and u_4 on the zoster infection.

From the finding collected from Fig. 18 gives a comprehensive insight into the biological interpretation when all the possible control measures are use simultaneously to individuals infected with varicella-zoster virus. Therefore, the combined implementation of all the proposed control strategies is pivotal for effectively curtailing varicella-zoster infections that spreads in the community. Furthermore, it gives highlights for the stakeholders that each control measure targets specific aspects such as protection, recovery enhancement, and treatment, working synergistically to reduce the number of varicella-zoster infection. Thus, this holistic approach acknowledges the intricate nature of varicella-zoster infection dynamics and underscores the significance of a multifaceted intervention strategy in managing and controlling varicella-zoster infection in the community.

In this part, we carried out numerical simulation to investigate and discussed the impacts of the control strategies used to simulate Figs. 19 and 20 respectively. The finding from Fig. 19 reveals that the impact of implementing the control measures u_3 and u_4 on the co-infection that shows a decline in the co-infected population. Similarly, the finding from Fig. 20 reveals that the impacts of the combined implementation of u_3, u_4 and u_5, that indicate a more substantial decrease in co-infection compared to the implementation of the controls u_3 and u_4. Thus, utilizing u_3, u_4 and u_5 simultaneously is the most strong strategy to undertake the co-infection. This offers valuable insights for creating comprehensive interventions to manage the dynamics of the co-infected population.

Fig. 21 explains the biological consequences of implementing all the proposed control measures simultaneously on individuals co-infected with HIV/AIDS and varicella-zoster. The results underscore the pivotal role of a comprehensive intervention strategy in addressing co-infection. By integrating measures to prevent HIV and Varicella-Zoster, improve recovery, and offer treatment for co-

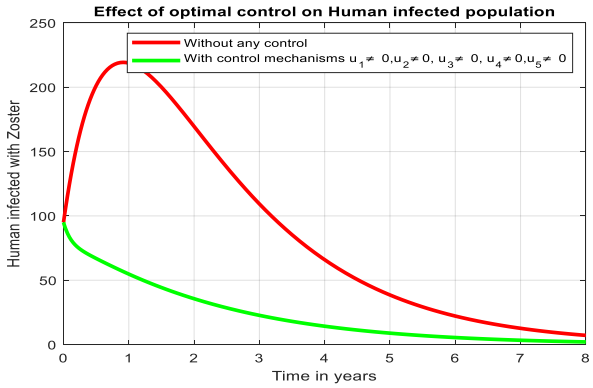

Fig. 18. Simulation result to reveals the impact of all the control measures on the zoster infection.

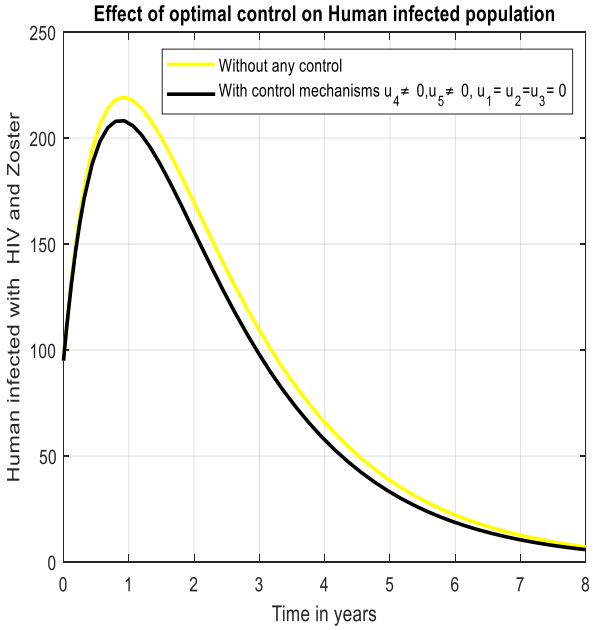

Fig. 19. Simulation result to reveals the impacts of the control measures u_4 and u_5 on the co- Infected infection.

infections, the figure demonstrates a significant decrease in the co-infected population. From a biological standpoint, this highlights the importance of a multifaceted approach that addresses various aspects of infection dynamics concurrently. These findings suggest that a holistic strategy, incorporating multiple control measures, is crucial for effectively managing and mitigating the impact of co-infections, providing valuable insights for public health interventions.

6. Conclusions and recommendations

This proposed study built up an integer model integrating five time-dependent optimal control strategies to scrutinize the dynamics of HIV/AIDS and varicella-zoster co-infection spreading in the community. Rigorous assessment of the model's equilibrium points is conducted to ensure its mathematical and epidemiological robustness. The models associated reproduction numbers are computed, and sensitivity analysis was performed to gauge the influence of the model parameters variations on the co-infection disease propagation.

Then the sensitivity analysis and the various numerical simulations are carried out to explore the impacts of slight parameter fluctuations on the reproduction number and the model state variables. The results underscore the efficacy of medication and treatment of zoster-only cases in reducing both HIV/AIDS and zoster co-infection within the community. Furthermore, modifying the zoster vaccination coverage emerges as a critical prophylactic measure, significantly curtailing the frequency of both infectious diseases. Based on these visible findings of the numerical simulation, the following recommendations are proposed: Achieving a zoster vaccination rate exceeding one-third is imperative for eliminating the HIV/AIDS and varicella co-infection in the community, consideration to reducing the zoster vaccination portion by over four-fifths as a potential control measure for the HIV/AIDS and

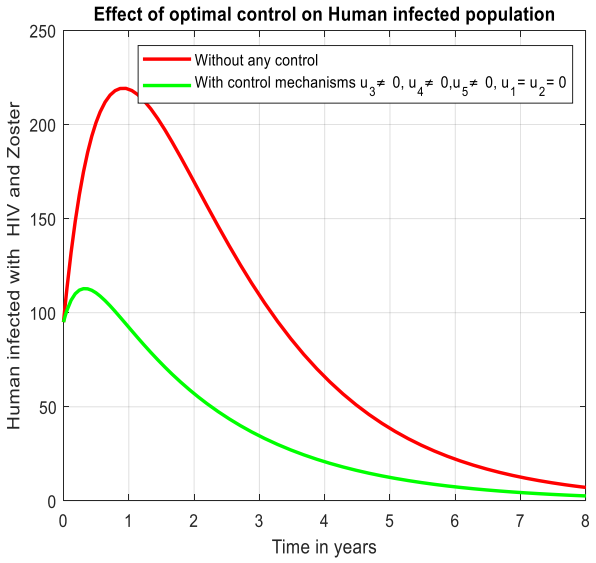

Fig. 20. Simulation result to reveals the impacts of the control measures u_3, u_4 and u_5 on the infection.

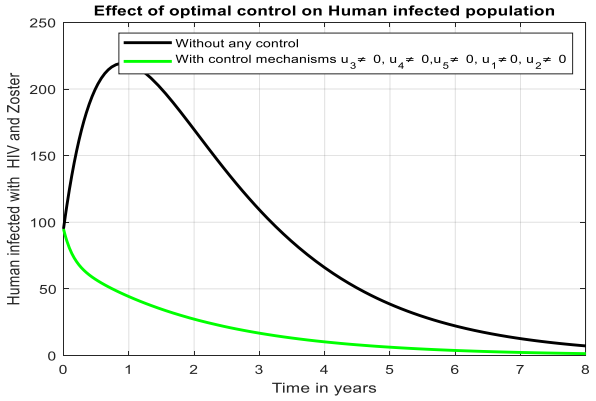

Fig. 21. Impact of implementing all the possible control strategies simultaneously on the HIV/AIDS and varicella-zoster co-infection.

varicella co-infection management, vaccine coverage surpassing one-third is essential to mitigate all the three illnesses, prioritizing the reduction of the spreading rate by more than one-third is crucial for controlling the spread of the HIV/AIDS and varicella co-infection. This study underscores the practical impact of pharmaceutical interventions in reducing HIV/AIDS and varicella co-infection. Moreover, modifying the access to the zoster vaccine emerges as a pivotal prophylactic measure, with numerical simulation results demonstrating its tangible impact on minimizing the disease frequency within communities. These outcomes bolster the case for vaccination programs and highlight the real-world implications of public health measures.

Finally, the numerical simulation performed for the optimal control problem model has yielded significant insights into the spreading dynamics of HIV/AIDS and varicella-zoster co-infection. The control measures $(u_1, u_2, u_3, u_4,$ and $u_5)$ we have introduced in the co-infection model (4) play crucial roles in protecting against the HIV/AIDS or varicella-zoster infections, enhancing recovery, and declining the treated co-infected individuals. The detailed examination of particular and combined control measures highlights their impacts in reducing the respective infected population and mitigating HIV/AIDS and varicella-zoster co-infection. Looking ahead, exploring stochastic or fractional order approaches with cost-effectiveness analysis could enhance the model's accuracy and capture more complex real-world scenarios. Such advancements could provide valuable insights for public health practices and intervention planning, advance our understanding of co-infection dynamics and optimal control strategies.

Funding

There is no fund for this research study.

Availability of data

No data was used for this research and all details about our research are included in the article.

CRediT authorship contribution statement

Belela Samuel Kotola: Writing – review & editing, Writing – original draft, Visualization, Validation, Supervision, Software, Resources, Project administration, Methodology, Investigation, Funding acquisition, Formal analysis, Data curation, Conceptualization. **Shewafera Wondimagegnhu Teklu:** Writing – review & editing, Validation, Investigation, Data curation.

Declaration of competing interest

The authors wish to declare that no specific financial or non-financial support was provided by any third party for the work reported in this manuscript. Additionally, none of the authors have received consulting fees, honoraria, or any other financial benefits from entities related to the subject matter of this manuscript within the past three years. Furthermore, none of the authors hold any patents, copyrights, or other intellectual property rights relevant to the work described in this manuscript. We affirm that there are no other potential competing interests that could influence the outcomes or interpretations presented in this study.

References

[1] Derek L. Carbaugh, Helen M. Lazear, Flavivirus envelope protein glycosylation: impacts on viral infection and pathogenesis, J. Virol. 94 (11) (2020) 10–1128.
[2] M.S.1 Nassar, M.A. Bakhrebah, Sultan Ayoub Meo, M.S. Alsuabeyl, W.A. Zaher, Middle East Respiratory Syndrome Coronavirus (MERS-CoV) infection: epidemiology, pathogenesis and clinical characteristics, Eur. Rev. Med. Pharmacol. Sci. 22 (15) (2018) 4956–4961.
[3] T. Evans-Gilbert, Vertically transmitted chikungunya, Zika and dengue virus infections: the pathogenesis from mother to fetus and the implications of co-infections and vaccine development, International Journal of Pediatrics and Adolescent Medicine 7 (3) (2020) 107–111.
[4] Anne M. Lachiewicz, Megan L. Srinivas, Varicella-zoster virus post-exposure management and prophylaxis: a review, Preventive medicine reports 16 (2019) 101016.
[5] Peter GE. Kennedy, Anne A. Gershon, Clinical features of varicella-zoster virus infection, Viruses 10 (11) (2018) 609.
[6] Kerry J. Laing, JD Ouwendijk Werner, David M. Koelle, Georges MGM. Verjans, Immunobiology of varicella-zoster virus infection, J. Infect. Dis. 218 (suppl_2) (2018) S68–S74.
[7] János Karsai, Rita Csuma-Kovács, Ágnes Dánielisz, Zsuzsanna Molnár, János Dudás, Teodóra Borsos, Gergely Röst, Modeling the transmission dynamics of varicella in Hungary, Journal of Mathematics in Industry 10 (1) (2020) 12.
[8] Anant Patil, Mohamad Goldust, Uwe Wollina, Herpes zoster: a review of clinical manifestations and management, Viruses 14 (2) (2022) 192.
[9] Peter GE. Kennedy, Trine H. Mogensen, Determinants of neurological syndromes caused by varicella zoster virus (VZV), J. Neurovirol. 26 (2020) 482–495.
[10] Firaol Asfaw Wodajo, Temesgen Tibebu Mekonnen, Effect of intervention of vaccination and treatment on the transmission dynamics of HBV disease: a mathematical model analysis, J. Math. 2022 (2022).
[11] Varicella-Zoster Virus Reactivation and Increased Vascular Risk in People Living with HIV: Data from a Retrospective Cohort Study.
[12] Varicella-zoster Virus Reactivation Is Frequently Detected in HIV-infected Individuals Presenting with Stroke.
[13] Shewafera Wondimagegnhu Teklu, Belela Samuel Kotola, A dynamical analysis and numerical simulation of COVID-19 and HIV/AIDS co-infection with intervention strategies, J. Biol. Dynam. 17 (1) (2023) 2175920.
[14] Shewafera Wondimagegnhu Teklu, Yohannes Fissha Abebaw, Birhanu Baye Terefe, Dejen Ketema Mamo, HIV/AIDS and TB co-infection deterministic model bifurcation and optimal control analysis, Inform. Med. Unlocked 41 (2023) 101328.
[15] Robert W. Eisinger, Carl W. Dieffenbach, Anthony S. Fauci, HIV viral load and transmissibility of HIV infection: undetectable equals untransmittable, JAMA 321 (5) (2019) 451–452.
[16] Belela Samuel Kotola, Shewafera Wondimagegnhu Teklu, Yohannes Fissha Abebaw, Bifurcation and optimal control analysis of HIV/AIDS and COVID-19 co-infection model with numerical simulation, PLoS One 18 (5) (2023) e0284759.
[17] Shewafera Wondimagegnhu Teklu, Birhanu Baye Terefe, Dejen Ketema Mamo, Yohannes Fissha Abebaw, Optimal control strategies on HIV/AIDS and pneumonia co-infection with mathematical modelling approach, J. Biol. Dynam. 18 (1) (2024) 2288873.
[18] Shewafera Wondimagegnhu Teklu, Koya Purnachandra Rao, HIV/AIDS-Pneumonia Codynamics model analysis with vaccination and treatment, Comput. Math. Methods Med. 2022 (2022).
[19] Ibrahim M. Hezam, Abdelaziz Foul, Alrasheedi Adel, A dynamic optimal control model for COVID-19 and cholera co-infection in Yemen, in: Advances in Difference Equations 2021, 2021, pp. 1–30, 1.
[20] Shewafera Wondimagegnhu Teklu, Investigating the effects of intervention strategies on pneumonia and HIV/AIDS Coinfection model, BioMed Res. Int. 2023 (2023).
[21] Belela Samuel Kotola, Dawit Melese Gebru, Haileyesus Tessema Alemneh, Appraisal and simulation on Codynamics of pneumonia and Meningitis with vaccination intervention: from a mathematical model perspective, Comput. Math. Methods Med. 2022 (2022).
[22] Tibebu Mekonnen Temesgen, Belela Samuel Kotola, "Mathematical model analysis and numerical simulation for codynamics of meningitis and pneumonia infection with intervention.", Scientific Reports 12 (1) (2022) 2639.
[23] Mohammed Kizito, Julius Tumwiine, A mathematical model of treatment and vaccination interventions of pneumococcal pneumonia infection dynamics, J. Appl. Math. 2018 (2018).
[24] M. Comba, S. Martorano-Raimundo, Ezio Venturino, A cost-effectiveness-assessing model of vaccination for varicella and zoster, Math. Model Nat. Phenom. 7 (3) (2012) 62–77.
[25] S.Y. Tchoumi, M.L. Diagne, H. Rwezaura, J.M. Tchuenche, Malaria and COVID-19 co-dynamics: a mathematical model and optimal control, Appl. Math. Model. 99 (2021).
[26] Shewafera Wondimagegnhu Teklu, Abebe Addise Meshesha, Saif Ullah, Analysis of tinea capitis epidemic fractional order model with optimal control theory, Inform. Med. Unlocked 42 (2023) 101379.
[27] Banan Maayah, Asma Moussaoui, Samia Bushnaq, Omar Abu Arqub, The multistep Laplace optimized decomposition method for solving fractional-order coronavirus disease model (COVID-19) via the Caputo fractional approach, Demonstr. Math. 55 (1) (2022) 963–977.
[28] Banan Maayah, Omar Abu Arqub, Salam Alnabulsi, Hamed Alsulami, Numerical solutions and geometric attractors of a fractional model of the cancer-immune based on the Atangana-Baleanu-Caputo derivative and the reproducing kernel scheme, Chin. J. Phys. 80 (2022) 463–483.
[29] Shewafera Wondimagegnhu Teklu, Belela Samuel Kotola, Insight into the treatment strategy on pneumonia transmission with asymptotic carrier stage using fractional order modelling approach, Computer Methods and Programs in Biomedicine Update (2024) 100134.

[30] Shewafera Wondimagegnhu Teklu, Abebe Addise Meshesha, Saif Ullah, Analysis of optimal control strategies on the fungal Tinea capitis infection fractional order model with cost-effective analysis, Sci. Rep. 14 (1) (2024) 1508.
[31] Ausif Padder, Laila Almutairi, Sania Qureshi, Amanullah Soomro, Afroz Afroz, Evren Hincal, Asifa Tassaddiq, Dynamical analysis of Generalized Tumor model with caputo fractional-order derivative, Fractal and Fractional 7 (3) (2023) 258.
[32] Abdullahi Yusuf, Sania Qureshi, Umar T. Mustapha, Salihu S. Musa, Tukur A. Sulaiman, Fractional modeling for improving scholastic performance of students with optimal control, International Journal of Applied and Computational Mathematics 8 (1) (2022) 37.
[33] Bernd J. Schroers, Ordinary Differential Equations: a Practical Guide, Cambridge University Press, 2011.
[34] Horst R. Thieme, Mathematics in Population Biology, vol. 1, Princeton University Press, 2018.
[35] Shewafera Wondimagegnhu Teklu, Analysis of fractional order model on higher institution students' anxiety towards mathematics with optimal control theory, Sci. Rep. 13 (1) (2023) 6867.
[36] Pauline Van den Driessche, James Watmough, Reproduction numbers and sub-threshold endemic equilibria for compartmental models of disease transmission, Math. Biosci. 180 (1–2) (2002) 29–48.
[37] D. Grass, J.P. Caulkins, G. Feichtinger, G. Tragler, D.A. Behrens, Optimal Control of Nonlinear Processes, with Applications in Drugs, Corruption, and Terror, Springer, Berlin/Heidelberg, Germany, 2008.
[38] W.H. Fleming, R.W. Rishel, Deterministic and stochastic optimal control, Appl. Math. 1 (1976).
[39] V. Barbu, T. Precupanu, Convexity and Optimization in Banach Spaces, fourth ed., Springer, Dordrecht, The Netherlands, 2010.
[40] K.R. Fister, S. Lenhart, J.S. McNally, Optimizing chemotherapy in an hiv model, Electron. J. Differ. Equ. 1998 (32) (1998) 1–12.
[41] E.A. Coddington, N. Levinson, Theory of Ordinary Differential Equations, McGraw Hill Co. Inc., New York,NY, USA, 1955.
[42] V. Barbu, T. Precupanu, Convexity and Optimization in Banach Spaces, fourth ed., Springer, Dordrecht, The Netherlands, 2010, p. 42.
[43] Baba Seidu, D. Makinde Oluwole, Optimal control of HIV/AIDS in the workplace in the presence of careless individuals, Computational and Mathematical Methods in Medicine 2014 (2014).